https://doi.org/10.5194/acp-2019-821
Preprint. Discussion started: 8 October 2019

Atmospheric Chemistry and Physics Discussions

Evaluation of the CAMS global atmospheric trace gas reanalysis 2003-2016 using aircraft campaign observations

Yuting Wang[1,6,*], Yong-Feng Ma[2,6] Henk Eskes[3], Antje Inness[4], Johannes Flemming[4], Guy P. Brasseur[1,5]

[1]Max Planck Institute for Meteorology, Hamburg, 20146, Germany
[2]Institute of Geophysics, faculty of Physics, University of Warsaw, Poland
[3]Royal Netherlands Meteorological Institute, De Bilt, The Netherlands
[4]ECMWF, Shinfield Park, Reading, RG2 9AX, UK
[5]National Center for Atmospheric Research, Boulder, CO, USA
[6]These two authors contributed equally to this work.

Correspondence to: Guy Brasseur (guy.brasseur@mpimet.mpg.de)

**Now at Department of Civil and Environmental Engineering, the Hong Kong Polytechnic University, Hung Hom, Kowloon, Hong Kong*

Abstract. The Copernicus Atmosphere Monitoring Service (CAMS) operated by the European Centre for Medium Range Weather Forecasts (ECMWF) has produced a global reanalysis of aerosol and reactive gases (called CAMSRA) for the period 2003-2016. Space observations of ozone, carbon monoxide, NO_2 and aerosol optical depth are assimilated by a 4-D Var method in the 60-layer ECMWF global atmospheric model, which for the reanalysis is operated at a horizontal resolution of about 80 km. As a contribution to the evaluation of the reanalysis, we compare atmospheric concentrations of different reactive species provided by the CAMS reanalysis with independent observational data gathered by airborne instrumentation during the field campaigns INTEX-A, INTEX-B, NEAQS-ITCT, ITOP, AMMA, ARCTAS, VOCALS, YAK-AEROSIB, HIPPO and KORUS-AQ. We show that the reanalysis reproduces rather successfully the observed concentrations of chemical species that are assimilated in the system including O_3 and CO with the biases generally less than 20 %, but generally underestimate the concentrations of the primary hydrocarbons and secondary organic species. In some cases, large discrepancies also exist for fast-reacting radicals such as OH and HO_2.

1 Introduction

Global reanalyses of the chemical composition of the atmosphere are intended to provide a detailed and realistic view of the three-dimensional distribution and evolution of the concentrations of the chemical species over a period of several years. Information provided by advanced models in which different observational data are assimilated, is provided at rather high spatial and temporal resolutions (typically 80-110 km and 3-6 hours, respectively). The Copernicus Atmosphere Monitoring Service (http://atmosphere.copernicus.eu, CAMS), operated by the European Centre for Medium Range Weather Forecasts

https://doi.org/10.5194/acp-2019-821
Preprint. Discussion started: 8 October 2019

Atmospheric Chemistry and Physics Discussions

(ECMWF) on behalf of the European commission, is currently producing a new global reanalysis of aerosols and reactive trace gases (referred to as CAMSRA). The current released reanalysis of aerosols and reactive gases covers the period 2003-2016 (Inness et al., 2019; Wagner et al., 2019), and has recently been extended to 2017 and 2018 (Christophe et al., 2019), and this reanalysis run will be continued close to real time. ECMWF has produced several other Atmospheric Composition (AC) reanalyses. The earlier Monitoring Atmospheric Composition and Climate (MACC) project produced the MACC reanalysis (MACCRA) for the period of 2003-2012 (Inness et al., 2013; Stein et al., 2012). The CAMS interim reanalysis (CIRA) is a test product implemented after the retirement of the coupled Integrated Forecast System (IFS-MOZART; Flemming et al., 2009) and its replacement by the IFS with on-line integrated chemistry and aerosol schemes ((Flemming et al., 2015). The CIRA is available from 2003 to 2018 (Flemming et al., 2017). The CAMSRA is built on the experience gained during the production of these previous two versions of the reanalysis, MACCRA and CIRA.

The validation of the CAMSRA is routinely performed by the CAMS validation team through the CAMS-84 contract co-ordinated by KNMI (Christophe et al., 2019; Eskes et al., 2015, 2018). The validation uses various measurements, including satellite observations, ground-based remote sensing and in-situ measurements, ozone soundings and commercial aircraft measurements, to assess the performance of the model versions and the reanalysis. The validation results for CAMSRA 2003-2016 using these operational measurements are shown by Eskes et al. (2018) and Wagner et al. (2019). The purpose of our paper is to report on the validation of the CAMSRA by using aircraft measurements performed during past field campaigns in different parts of the world.

In contrast to the long-term operational monitoring, aircraft campaigns are designed to address specific scientific questions, and perform intensive measurements in a specific region during a limited period of time. Aircraft campaigns are therefore valuable supplements to evaluate the models and, in particular the reanalyses. Another advantage of intensive campaigns is that they provide the opportunity to measure the concentrations of the chemical species that are not operationally monitored. The observations of these additional species can be used to better investigate the performance of the models and in particular their ability to represent some complex physical and chemical processes (Emmons et al., 2000).

Ozone (O_3) and carbon monoxide (CO) are two of the main chemical species that are simulated in the three reanalyses (MACCRA, CIRA, and CAMSRA). Satellite measurements of these species are assimilated in these three reanalyses resulting in analyzed concentrations strongly forced by observations (Inness et al., 2019). Furthermore, ozone and CO are measured during most of the field campaigns. Knowledge of the distribution of these two species is key for understanding the role of the chemical and transport processes in the atmosphere. Ozone is a key indicator of the photochemical pollution. This molecule is produced in the atmosphere by the reactions between nitrogen oxides ($NO_X = NO + NO_2$), CO, and volatile organic compounds (VOCs) in the presence of sunlight. Hydrogen radicals ($HO_X = OH + HO_2$) play an important role in this nonlinear process (Jacob, 2000; Lelieveld and Dentener, 2000). The photolysis of ozone followed by the reaction of the resulting electronically

https://doi.org/10.5194/acp-2019-821
Preprint. Discussion started: 8 October 2019

Atmospheric Chemistry and Physics Discussions

65 excited oxygen atom with water vapor (H2O) represents the main sink of tropospheric O_3 (Sheel et al., 2016). Carbon monoxide, either emitted at the surface by incomplete combustion of fossil fuels and biomass burning (Fortems-Cheiney et al., 2011), or produced in the atmosphere as a result of the oxidation of hydrocarbons, is destroyed mainly by reaction with the OH radical (Pressman and Warneck, 1970). In this paper, we mainly evaluate the concentration of O_3 and CO produced by all the three reanalyses, by comparing them with atmospheric observations made along flight tracks during past field campaigns
70 (see Table 2 below). These comparisons are performed in different regions of the world.

Other chemical species (NO_X, HO_X, organics) produced by the CAMSRA are also evaluated at selected locations. The hydrocarbons considered are ethene (C_2H_4), ethane (C_2H_6) and propane (C_3H_8). Secondary organic compounds, including methanol (CH_3OH), acetone (CH_3COCH_3), ethanol (C_2H_5OH), and methyl hydroperoxide (CH_3OOH), are the products of
75 hydrocarbons and CO oxidation. Peroxyacetyl nitrate (PAN) and nitric acid (HNO_3) are produced by photochemical reactions involving NO_X (Emmons et al., 2000). Hydrogen peroxide (H_2O_2) represents a major tropospheric sink for HO_X radicals. Formaldehyde (HCHO) is mainly produced by the oxidation of hydrocarbons, but also directly emitted to the atmosphere from industry sources; it has a substantial impact on the HO_X concentration. By comparing these species, the underlying processes in the model can be further evaluated.

80 **2 Model description**

Three versions of the global reanalysis are evaluated by conducting a comparison of the calculated fields with available measurements made from aircraft during selected field campaigns. Some of the key setups of these three reanalyses are listed in Table 1. More details can be found in Inness et al. (2019). MACCRA covers the period 2003 to 2012, while CIRA and CAMSRA provide three-dimensional global fields from 2003 to 2016. Thus, in our analysis, the campaigns that took place
85 after 2012 are excluded when compared to MACCRA. The model resolution for MACCRA and CAMSRA is equal to 80 km, while it is equal 110 km in the case of CIRA. All three reanalyses are made with a 60 vertical levels model and extend from the surface to 0.1 hPa. Each reanalysis provides two different outputs: an analysis and a 0-24 h forecast. These two fields were compared in the case of CAMSRA, and they appear to be very similar (not shown here). To be consistent in time resolution, the forecast fields are used in this work for all three reanalyses. An additional control run for CAMSRA without data
90 assimilation is also evaluated to separate the impact of the assimilation from the other model-related factors. The satellite datasets that are assimilated in CAMSRA are summarized in Table 2.

When comparing the concentrations calculated in the reanalyses with the campaign data, the 4D model grid points (space and time) that are considered are those that are closest to the measurement locations (latitude, longitude, and pressure layer) and
95 times.

https://doi.org/10.5194/acp-2019-821
Preprint. Discussion started: 8 October 2019

Atmospheric Chemistry and Physics Discussions

3 Aircraft measurements

Several aircraft campaigns are used to validate the three CAMSRA presented above. These campaigns are briefly described below, and in Table 2.

INTEX-A (Intercontinental Chemical Transport Experiment – North America Phase A) was an integrated atmospheric field experiment performed over the east coast of the United States organized by NASA during July and August in 2004 (Singh et al., 2006). It has contributed to a large ICARTT program (International Consortium for Atmospheric Research on Transport and Transformation; Fehsenfeld et al., 2006). During this campaign, the chemical species were measured by different instruments on board of a DC-8 air plane. The measurement methodology of the trace gases can be found in Singh et al. (2006).

NEAQS-ITCT (New England Air Quality Study – Intercontinental Transport and Chemical Transformation) was the NOAA component to the ICARTT program. The instruments were setup on a WP-3D aircraft, and the details can be found by Fehsenfeld et al. (2006).

ITOP (Intercontinental Transport of Pollution) was the European (U. K., Germany, and France) contribution to ICARTT project. In the present study, we collect the measurements made on board of the UK FAAM BAE-146 aircraft. The instrument information is provided by Cook et al. (2007).

INTEX-B (Intercontinental Chemical Transport Experiment – Phase B) was the second phase of the INTEX-NA experiment led by NASA. In March of 2006, INTEX-B operated in support of the multi-agency MIRAGE/MILAGRO (The Megacity Initiative: Local and Global Research Observations; Molina et al., 2010) project with a focus on observations in and around Mexico City. In its second phase, INTEX-B focused on the east coast of U. S. and on the Pacific Ocean during the spring of 2006 (Singh et al., 2009). The NCAR component of MILAGRO was MIRAGE-Mex (Megacities Impact on Regional and Global Environment), and NCAR also contributed to INTEX-B. The NASA measurement platform was the DC-8 research aircraft. The measurement approaches for the selected species were the same as those adopted for INTEX-A. The NCAR measurements were made from the NSF/NCAR C-130 airplane. The measurement method is described by Singh et al. (2009).

AMMA (African Monsoon Multidisciplinary Analysis) was an international project to improve our knowledge and understanding of the West African monsoon (Lebel et al., 2010). Measurements to investigate the chemical composition of the middle and upper troposphere in West Africa during July to August 2006 campaign were performed by the U. K. FAAM BAE-146 aircraft, and the details are described by Saunois et al. (2009).

https://doi.org/10.5194/acp-2019-821
Preprint. Discussion started: 8 October 2019

Atmospheric Chemistry and Physics Discussions

ARCTAS (Arctic Research of the Composition of the Troposphere from Aircraft and Satellites) was conducted during April and July 2008 by NASA (Jacob et al., 2010). ARCTAS was part of the international POLARCAT program during the 2007-2008 International Polar Year (IPY). In the present study, we use the measurements made on board of NASA DC-8 research aircraft. The species measured during ARCTAS were the same as during INTEX-A.

VOCALS (VAMOS Ocean-Cloud-Atmosphere-Land Study) was an international program that is part of the CLIVAR VAMOS (Variability of the American Monsoon Systems) project. The VOCALS experiment was conducted from 15 October to 15 November 2008 in the Southeast Pacific region (Allen et al., 2011). The NSF C-130 aircraft was used during the campaign.

YAK-AEROSIB (Airborne Extensive Regional Observations in Siberia) was a bilateral cooperation activity coordinated by researchers from LSCE in France and IAO in Russia. It aims to establish systematic airborne observations of the atmospheric composition over Siberia. In the present study, we used the O_3 and CO measurements during 2006 - 2008 and in 2014. The program used a Tupolev Tu-134 aircraft. The detailed measurement techniques can be found in Paris et al. (2008; 2010).

HIPPO (HIAPER Pole-to-Pole Observations), supported by NSF and operated by NCAR, used the NSF/NCAR G-V aircraft. During five missions from 2009 to 2011in different seasons, a large number of chemical species were observed between the Arctic and the Antarctic over the Pacific Ocean. The details can be found in Wofsy et al. (2012).

KORUS-AQ (Korea-US Air Quality Study) was a joint Korea and U. S. campaign that took place in South Korea from April to June 2016. The U. S. contribution was led by NASA, and the aircraft platform was the NASA DC-8. The species were measured as during the INTEX-A campaign. A further description of this field campaign can be found in the KORUS-AQ White Paper (https://espo.nasa.gov/korus-aq/content/KORUS-AQ_Science_Overview_0, last access: 10 July 2019).

Information of aircraft campaigns is summarized in Table 3. The flight tracks are shown in Figure 1.

4 Evaluation of spatial distributions of chemical species

In the present Section, we first evaluate the CAMSRA by comparing the calculated (reanalysed) and observed concentrations of ozone, carbon monoxide and other chemical species in different regions of the world during the selected field campaigns. Carbon monoxide and ozone were measured in all the field campaigns considered in the present study. Data are available in both hemispheres, but principally in the regions of North America, eastern Asia, Australia and across the Pacific Ocean. In the

https://doi.org/10.5194/acp-2019-821
Preprint. Discussion started: 8 October 2019

Atmospheric Chemistry and Physics Discussions

case of nitrogen oxides, hydroxyl and peroxyl radicals and formaldehyde, only the measurements provided in North America, the northern Pacific and eastern Asia are considered here.

4.1 Ozone

For the spatial evaluation, all the aircraft measurements and the extracted model data points are combined regardless the measurement time; the measurements and models are separated into three altitude layers: the low troposphere layer (0-3 km), the middle troposphere layer (3-9 km), and the upper troposphere/lower stratospheric layer (9-14 km).

The comparison of O_3 between the observation and the reanalyses is shown in Figure 2, 3, 4. The tropospheric ozone concentration is higher in the northern hemisphere than the southern hemisphere because of higher anthropogenic emissions of ozone precursors (air pollution). In the 9-14 km layer, the polar ozone concentrations are very high because the height of the tropopause in that region is lower than at lower latitudes, and as a result, the aircraft penetrated in the ozone-rich stratosphere. The comparison between the observation and the reanalysis values from MACCRA is generally good. In the low troposphere, the biases of the averaged grids are mostly within 20 %. MACCRA underestimates the O_3 concentrations in the Arctic region and in the southern hemisphere; while it overestimates the O_3 concentrations in the northern low and mid-latitudes, especially over the western Pacific Ocean (over 50 %), the eastern coast of U. S. and the North Atlantic (about 40 %). The biases of MACCRA in the middle troposphere are smaller than those in the low troposphere. The positive biases in the lower layer become smaller with increasing altitude everywhere except in the Arctic, where the negative biases turn to positive values. In the upper troposphere, the agreement is worse than in the lower layers. The biases are mostly positive over the Pacific Ocean and negative in North America.

The agreement of CIRA with the aircraft measurements is similar to the agreement of MACCRA when using the same measurements before 2013. In the lowest layer, however, the mean bias of CIRA is slight smaller than that of MACCRA. The CIRA reanalysis overestimates the observation in the middle of the Pacific Ocean and northwest of the Atlantic Ocean, which is similar to the values derived from MACCRA, but with smaller biases; CIRA underestimates ozone concentrations in the rest of the region with biases of less than 20 %. Above the Pacific Ocean, the positive bias, which is small in the lower layers of the atmosphere, increases with height and becomes substantial in the upper troposphere. The patterns of the biases in the CIRA reanalysis in the upper troposphere are similar to those in the middle troposphere layer, but with larger values.

The comparison of the flight campaign ozone concentrations with CAMSRA is also good. In the low troposphere, CAMSRA generally overestimates the O_3 concentration relative to the observation, which is different from the MACCRA and CIRA cases. The biases of CAMSRA are usually less than 15 %, and the relative larger biases are found in the tropics and Arctic, where the reanalysis overestimates the measurements by about 30 %. In the free troposphere, the biases of the reanalysis

https://doi.org/10.5194/acp-2019-821
Preprint. Discussion started: 8 October 2019

Atmospheric Chemistry and Physics Discussions

become larger than in the low troposphere, especially over the tropical ocean, while the differences are smaller in the western African region. For the comparison above 9 km, the positive biases over the Pacific Ocean are even larger and reach 50 %.

The mean bias of the CAMS control simulation (model run performed without assimilation of observed data) is similar to the bias associated with CAMSRA, but the patterns are different. The bias of CAMSRA is more uniform over the globe, which shows that data assimilation improves the global distribution of the O_3 concentration. In the low troposphere, the bias of the control run is of the order of 15 %. The control run underestimates the measurements in the west coast of U.S. and in the south of the Pacific Ocean, where the ozone concentrations provided by the CAMSRA are higher than the observation. In the polar free troposphere, the control simulation provides concentration values that are lower than suggested by the observations with a bias of about 20 %; in contrast to this, in the tropical region, the control simulation overestimates ozone, which is similar to the corresponding estimates by CAMSRA. In the upper layer, the bias pattern is similar to that in the free troposphere, but the bias values are larger.

Overall, for ozone, the level of agreement between the observations and the three reanalyses, and between the observations and the control run are similar, but the biases associated with CAMSRA are more uniform in space. A linear regression was performed between all observed ozone data points and ozone concentrations extracted from the three reanalyses and from the control simulation. Table 4 lists the corresponding linear regression parameters. Fewer data are available when considering MACCRA because MACCRA includes information only until year 2012. To more directly compare with MACCRA, the regression parameters for the other models runs before 2013 are also given in the table. The correlations of all the three reanalysis cases are high with squared correlation coefficients larger than 0.9. The highest correlation is achieved with CAMSRA. The squared correlation coefficient R^2 derived for the control simulation (0.89) is not substantially smaller than in the three cases with assimilation (0.93). This suggests that the CAMS model in its control mode has good predictive capability, but that, as expected, data assimilation slightly improves the calculated ozone fields. To exclude the contribution of stratospheric ozone values in the statistical analysis, the stratospheric data were filtered out, and the statistical parameters recalculated. The squared correlation coefficients decreased from about 0.9-0.95 to about 0.6-0.7.

4.2 Carbon monoxide

The comparison of carbon monoxide between the observation and the reanalyses is shown in Figures 5, 6 and 7. MACCRA underestimates the CO concentrations in the Arctic region and Canada (about 30 %), west Africa (about 20 %), and the Southern Ocean (about 10 %). It overestimates the concentrations in the other regions covered by the campaigns with most of the biases within 15 %. In the middle troposphere, the bias pattern is similar to that of the low troposphere, but the biases are smaller than in the lowest layer, especially in the Arctic. In the upper layer, often located in the stratosphere, the biases become larger at high latitudes (positive in the Arctic and negative in the Southern Ocean), with the biases larger than 50 %. In this layer, the patterns of the biases over the Pacific Ocean are different than in the lower layers.

https://doi.org/10.5194/acp-2019-821
Preprint. Discussion started: 8 October 2019

Atmospheric Chemistry and Physics Discussions

CIRA agrees better with the observations than MACCRA. In the low troposphere, the biases are smaller than those derived with MACCRA, and the large negative biases in the Arctic found in MACCRA disappear with CIRA. The mean bias of CIRA is only of the order of 10 %. CIRA underestimates the CO observation in the region of the northern Pacific Ocean, but MACCRA overestimates the concentrations there. In the middle troposphere, CIRA underestimates CO in most regions in the northern hemisphere, while it overestimates CO in the southern hemisphere. In the upper layer, the biases of CIRA are also large at high latitudes, but the biases are positive in the both polar regions.

The agreement between the CO measurements and the CAMSRA is generally good with biases generally smaller than 15 %. In the low and middle troposphere, the CAMSRA behaves similarly to CIRA; however, in the upper layer, the biases are different. The biases in CAMSRA become smaller in the polar region. CAMSRA underestimates CO concentrations in most regions of the low and mid latitudes with biases less than 20 %.

The bias between the control run and the CO observations is larger than for the CAMSRA. The bias pattern of the control run in the lowest layer is similar to that of CAMSRA, but the positive biases in the southern hemisphere are larger (about 30 %). In the free troposphere, the control run underestimates the CO concentration at latitudes north of 40 °N, similar to the CAMSRA, but overestimates the CO elsewhere. The positive model biases in the southern hemisphere and tropics are efficiently removed by the assimilation of CAMSRA. In the upper layer, the biases are positive in most regions except west of North America. The biases are large in the polar stratosphere, where they reach about 50 %.

When confronted with CO data collected by airborne instrumentation, all three reanalyses provide good results in the low and middle troposphere; however, the two early reanalyses are not successful when considering the field observations made in the polar region, specifically in the upper troposphere/lower stratosphere. The situation is improved with the new CAMSRA reanalysis. The control simulations performed without assimilation overestimate the CO concentration in the southern hemisphere. The linear regression parameters of CO are shown in Table 5. For all the data points, the correlations are weak due to the extreme values appearing in localized pollution plumes, not captured by coarse resolution global models. After filtering out these extreme values (values larger than 300 ppb), the correlations of CO between the observations and models improve substantially. The correlation calculated using CAMSRA is the highest with a correlation coefficient of 0.71 and a slope of 0.78.

4.3 Other chemical species

Spatial distributions of nitrogen oxides (NO_X = NO + NO_2), hydroxyl radical (OH), hydroperoxyl radical (HO_2), and formaldehyde (HCHO) for CAMSRA in the northern hemisphere are provided in the appendix. The CAMSRA reanalysis values are compared with observations from aircraft for three different layers of the atmosphere. Because the measurements

https://doi.org/10.5194/acp-2019-821
Preprint. Discussion started: 8 October 2019

Atmospheric Chemistry and Physics Discussions

of NO_X, OH, HO_2, and HCHO used in the work are only in North America, Arctic, and Korea, so the analysis below are for these regions.

In the case of NO_X, the CAMSRA reanalysis underestimates the values measured in the middle and upper troposphere, but overestimates the observed values in the lowest layer. There are several possible reasons: (1) the model overestimates the effect of regional pollution sources; (2) the model underestimates the local productions (e.g. lightning); (3) the model underestimates the convective transport; (4) the model underestimates the lifetime of the surface emissions. We also compared the NO_X between CAMSRA and the control run since NO_2 is assimilated in CAMSRA, but they are very similar, which means the assimilation did not improve the reanalysis of NO_X. In the case of HCHO, the reanalysis underestimates the observed concentrations at all levels. The negative biases in the low troposphere are between 20-40 %, while those in the higher levels are about 50 %. In the case of OH, the calculated values are overestimated at mid and low latitudes, which may lead to a shorter lifetime of NO_2, consistent with the vertical distribution of NO_X discussed above. CAMSRA underestimates OH concentrations in the Arctic region, and thus underestimates the chemical loss of CO in the Arctic stratosphere, and explains the overestimation of CO in that region. Finally, no clear pattern is found in the difference between model simulated values and observations of HO_2.

5 Evaluation of vertical profiles at selected locations

The CAMS reanalysis provides the global distribution of a large number of chemical species that are not directly assimilated by the CAMS system, but whose concentrations are calculated consistently with the assimilated species, ozone, carbon monoxide and nitrogen dioxide. We evaluate several key species calculated by CAMSRA at four selected locations with observations from NASA campaigns (INTEX-A in 2004, INTEX-B in 2006, and ARCTAS in 2008) that took place with the DC-8 research aircraft (Figure 8). These campaigns provide information on the atmospheric abundance of several reactive gases related to ozone and CO chemistry. The vertical profiles at the chosen locations are averaged based on ARCTAS campaign in the case of the Arctic region (measurements north to 60 °N), on the INTEX-B campaign in the case of Hawaii and Mexico and on INTEX-A in the case of the Bangor data. Since only O_3, CO, and NO_2 are assimilated in CAMSRA reanalysis, the control simulation without assimilation is shown only for O_3, CO, and NO_X. A comparison between the reanalysis and the control simulations for species other than O_3, CO and NO_X is not shown because the differences between the two runs are very small. The vertical profiles of ozone, carbon monoxide, nitrogen oxides (NO_X), hydroxyl (OH) and hydroperoxyl (HO_2) radical, formaldehyde (HCHO), hydrogen peroxide (H_2O_2), nitric acid (HNO_3), peroxyacetyl nitrate (PAN), ethene (C_2H_4), ethane (C_2H_6), propane (C_3H_8), methanol (CH_3OH), acetone (CH_3COCH_3), methyl hydroperoxide (CH_3OOH) and ethanol (C_2H_5OH) are shown in Figures 9, 10, 11, and 12.

https://doi.org/10.5194/acp-2019-821
Preprint. Discussion started: 8 October 2019

Atmospheric Chemistry and Physics Discussions

We first examine the case of the three assimilated species. In general, the profiles calculated with assimilated observations are in good agreement with the profiles observed by airborne instruments. There are some interesting points to note, however.

5.1 Ozone

In the case of ozone in the Arctic (Figure 9), where the vertical profile is strongly affected by stratospheric processes, the control run underestimates the O_3 concentration above 1 km and particularly above 6 km altitude. The assimilation brings the profile much closer to the aircraft data. The concentrations calculated by the control and the reanalysis runs in the surface layer below 1 km are almost twice as large as those derived from the observations, which may be affected by the halogen chemical removal in Arctic spring. In the free troposphere and low stratosphere, the agreement is best for CAMSRA. In Bangor (Figure 10), the control and reanalysis simulations underestimate the aircraft observations in the upper troposphere, while they overestimate the measurements near the surface.

The low-latitude ozone profiles (Figures 11 and 12) are well reproduced by the reanalysis. However, the control run tends to overestimate ozone in Mexico-City and to a lesser extend in Hawaii. In this last region, the agreement of O_3 between the observations and models is quite good below 7 km: the biases are positive and smaller than 10 %, which is opposite to what is found in the Arctic. The reanalysis provides slightly better results than the control run. At higher altitudes the positive biases get larger and the CAMSRA data become worse than in the control run. In Mexico-City, the model represents well the ozone bulge that is detected by the airborne instruments at 2 to 3 km and is observed for most chemical species. At higher altitudes, the control model overestimates the ozone concentration; however, the bias is reduced by the CAMSRA assimilation.

5.2 Carbon monoxide

In the case of Arctic CO (Figure 9), the general agreement between the control and reanalysis runs and the observed profile is very good. The control run, however, slightly underestimates the CO concentration in the troposphere but overestimates it in the stratosphere. The assimilation does not change significantly or even increase the biases in troposphere CO in CAMSRA but decrease the positive biases in the stratosphere. In Bangor (Figure 10), both the control and the reanalysis simulations underestimate the observed concentrations by typically 10 ppb above 3 km altitude, but underestimate the surface concentrations. At low latitudes (Hawaii and Mexico, Figures 11 and 12), the control simulation overestimates the concentrations by about 10 ppb in the free troposphere, while CAMSRA underestimates the values observed from the DC-8 by 10 ppb. In Hawaii in the first 2 km above the surface, the control run provides concentrations that are about 10 % lower than the aircraft observation. In Mexico, the control model provides surface values that are 30 % higher than the observation. The bulge observed at 2-3 km altitude is not reproduced by the model.

https://doi.org/10.5194/acp-2019-821
Preprint. Discussion started: 8 October 2019

Atmospheric Chemistry and Physics Discussions

5.3 Nitrogen oxides

In the Arctic (Figure 9) the control run underestimates the NO_X, especially above 8 km, i.e., in the layers strongly influenced by the injection of stratospheric air. The assimilation process does not substantially reduce the discrepancy, since the CAMS model does not include a detailed representation of stratospheric chemistry and NO_X in the stratosphere is strongly underestimated because of this. In Bangor (Figure 10), the models underestimate the NO_X above 2 km as in Arctic, but overestimate the NO_X below 2 km. In the low latitude regions (Mexico and Hawaii, Figures 11 and 12), the calculated profiles are in rather good agreement with the observations, except below 2 km, where the influence from local air pollution is not well captured by the control and reanalysis simulations. In Hawaii, the model tends to slightly underestimate the observation. As in the Arctic, this underestimation is larger in the case of the reanalysis. In all regions except the Arctic, the models provide higher surface concentrations than suggested by the measurements.

5.4 Hydroxyl and hydroperoxyl radicals

In the Arctic (Figure 9), the model underestimates OH concentrations by about 0.02 ppt at all altitudes (of the order of 50 %). Because OH is the main sink of CO in the stratosphere, the CO loss must be too weak in the model, which could contribute to the slight overestimation of stratospheric CO in the control run. In the reanalysis, the concentrations of HO_2 are overestimated by about 1 pptv between 4 and 8 km altitude. In Bangor (Figure 10), the reanalysis overestimates OH by about 0.2 pptv, which contributes to the underestimation of the CO concentration at this location. The HO_2 concentrations are overestimated by 3-5 pptv. In Hawaii, the simulations made for the reanalysis overestimate the OH concentrations below 6 km but underestimates them above 8 km, which is consistent to the overestimation of high-altitude CO in the control run. In Mexico-city, the simulated OH concentrations are larger than the measurements below 8 km, but smaller above 8 km. The reanalysis overestimates HO_2 by about 4 pptv or 20 %.

5.5 Hydrogen peroxide

In the Arctic (Figure 9), where the calculated concentrations of HO_2 are too high in CAMSRA, the concentration of hydrogen peroxide is overestimated by typically a factor 2. In Bangor (Figure 10), the overestimation is of the order of 20 %. The agreement between reanalysis and observations is generally good in Hawaii (Figure 11) and Mexico-City (Figure 12), except in the lower levels of the atmosphere, where the model overestimates the concentrations.

5.6 Nitric acid

Nitric acid concentrations are strongly affected by wet scavenging in the troposphere and, at high latitudes, by the downward flux of stratospheric air (Murphy and Fahey, 1994; Wespes et al., 2007). The reanalysis generally underestimates the concentration of HNO_3 above 2 km altitude. This is the case in the Arctic (Figure 9), in Bangor (Figure 10) and in Hawaii (Figure 11). The discrepancy is particularly large in the upper levels of the Arctic, which implies that (1) scavenging of HNO_3

https://doi.org/10.5194/acp-2019-821
Preprint. Discussion started: 8 October 2019

Atmospheric Chemistry and Physics Discussions

is too strong, (2) the reactive nitrogen (e.g. NO_X) in the stratosphere is too low due to missing stratospheric chemistry. The model accounts for the high concentrations observed in the lowest levels of the atmosphere, specifically in Mexico-city (Figure 12) and to a lesser extent in Bangor and Hawaii.

5.7 Peroxyacetyl nitrate (PAN)

The agreement between the calculated and observed PAN vertical profile is good in the Arctic (Figure 9), even though the concentrations are slightly underestimated between 2 and 8 km altitude. The agreement is also good in Hawaii (Figure 11) below 5 km altitude, but a discrepancy of about 50 % is found above this height. In Bangor (Figure 10), PAN concentrations are overestimated by about 25 % in the free troposphere and by as much as a factor 2 below 3 km altitude. The calculated concentrations are slightly too high in Mexico-city (Figure 12). The model shows the presence of a peak in the PAN concentration at 3 km, but the calculated concentrations values are somewhat too low.

5.8 Primary organic compounds: ethene (C_2H_4), ethane (C_2H_6) and propane (C_3H_8)

In most cases, the model underestimates the measured concentrations of the primary hydrocarbons, which indicates that the emissions are too low. The discrepancy is substantial at all altitudes for example for C_2H_4 in Hawaii (Figure 11), as well as C_3H_8 in the Arctic (Figure 9) and in Bangor (Figure 10). Calculated C_2H_6 is substantially lower than suggested by the observations at all four locations. In Mexico-city (Figure 12), the model reproduces rather successfully the vertical profile of C_2H_4, but underestimates C_3H_8 below 5 km altitude. This last compound is well represented in Hawaii in the upper troposphere, but is underestimated by the model below 7 km.

5.9 Secondary organic compounds: formaldehyde (HCHO), methanol (CH_3OH), acetone (CH_3COCH_3), ethanol (C_2H_5OH) and methyl hydroperoxide (CH_3OOH)

As should be expected from the underestimation by the reanalysis of the atmospheric concentration of the primary hydrocarbons, the model also underestimates the abundance of oxygenated organic species in the troposphere. This is the case in the Arctic (Figure 9), where the abundance of formaldehyde, acetone and ethanol are underestimated by typically factors 3 to 8. Methanol is too low by about 30 %. Large discrepancies are also found in Bangor (Figure 10) where methanol and acetone are underestimated by a factor 2 and methyl peroxide by a factor 5. In Hawaii (Figure 11), the concentration of formaldehyde is slightly underestimated in the middle and upper troposphere, but the discrepancy reaches a factor 2 at 2 km altitude. Methanol is underestimated by 30 % but acetone and ethanol are underestimated by a factor 2. The model is in better agreement with the observations in Mexico-City (Figure 12): this is the case for formaldehyde (except below 4 km where the calculated concentrations are a factor 3 too low), for methanol (except at the surface) and for methyl hydroperoxide except below 4 km. Ethanol is underestimated by a factor 2.

https://doi.org/10.5194/acp-2019-821
Preprint. Discussion started: 8 October 2019

Atmospheric Chemistry and Physics Discussions

To summarize the discussion, we have qualified the degree of success of the reanalysis model versus the observational vertical profiles in the 4 regions of the world that are considered in the present study. The results, based on a subjective comparison between the vertical profiles derived from the CAMSRA and the profiles measured independently by airborne instruments, are presented in the following table for the altitudes of 6 km above the ground and at the Earth's surface, respectively. The symbols used in this table are the following: G for good agreement (bias < 10 %), O for overestimation by the reanalysis model (10 % < bias < 40 %), and U for underestimation (-40 % < bias < -10 %). Double symbols (i.e., OO or UU) indicate from a subjective analysis that the disagreement is large (bias > 40 %).

6 Summary

Overall, the reanalysis of assimilated tropospheric chemical species such as ozone and carbon monoxide by the CAMSRA system reproduces rather satisfactorily the observations made independently from aircraft platforms during the analyzed campaigns that took place between 2004 and 2016.

In the case of ozone, the R^2 coefficient is close to 0.9 and the RMSE ranges between 21 and 26 ppbv, depending on the reanalysis case that is being considered. The values of the same coefficient in the control case (no assimilation) are 0.89 and 25.4 ppbv, respectively. When only tropospheric ozone data are considered, the R^2 coefficient is of the order of 0.61 to 0.69 and the RMSE is close to 11 ppbv. The corresponding values for the control case are 0.67 and 10.6 ppbv, respectively. In other words, the assimilation procedure improves, but only slightly, the value of the statistical coefficients that are derived. Note that the RMSE is reduced by a factor 2 when only the tropospheric data are used, and the R^2 coefficient are reduced by 20-30 percent.

In the case of carbon monoxide, the R^2 coefficient varies from 0.2 to 0.4 depending on the adopted reanalysis, and the RMSE ranges from 55 to 67 ppbv. When plumes are removed from the observational data, the R^2 coefficient increases to 0.6-0.7 and the RMSE is reduced to 23-25 ppbv. These values are not substantially different from the coefficients obtained when the observations are compared with the control runs. But the assimilation brought the simulated CO concentrations to more uniform global distribution, which is a success of the reanalysis system.

The CAMSRA reproduced the vertical profiles of O_3 and CO quite well at selected four locations. For the species largely affected by the local plume (e.g. CO and NO_X), the CAMSRA underestimated the peak values. The simulation of OH and HO_2 in CAMSRA is generally satisfactory, but in some case the disagreement is big. The CAMSRA generally underestimated the primary hydrocarbons and the secondary organic compounds at all locations, implying the emissions are too low in the inventory used by CAMS system.

https://doi.org/10.5194/acp-2019-821
Preprint. Discussion started: 8 October 2019

Atmospheric Chemistry and Physics Discussions

Data availability.

The data used for the analysis are available on line (see Table 3). The results of the analysis are available on request from the first author.

Author contributions.

Y.W. and Y-F.M. have equally contributed to this paper. They have performed the analysis of the data produced by the different field campaigns. G. P. B. has developed the project idea. H.E., A. I. and J. F. have provided ideas and comments on the study and are directly involved in the CAMS project supported by the European Commission. Y. W. and G. P. B. wrote the paper.

Competing interests.

The authors declare that they have no conflict of interest.

Acknowledgements.

The present work was funded through the CAMS-84 (CAMS validation) contract, coordinated by the Royal Netherlands Meteorological Organization (KNMI, Henk Eskes). The Copernicus Atmosphere Monitoring Service (CAMS) is operated by the European Centre for Medium-Range Weather Forecasts on behalf of the European Commission as part of the Copernicus Programme. We acknowledge all the investigators who have made the measurements and made them available online. We thank Jean-Daniel Paris (Laboratoire des Sciences du Climat et de l'Environnement, Gif sur Yvette, France) and Philippe Nédélec (Laboratoire d'Aérologie, Toulouse, France) for providing the YAK-AEROSIB campaign data. The National Center for Atmospheric Research is sponsored by the US National Science Foundation.

References

Allen, G., Coe, H., Clarke, A., Bretherton, C., Wood, R., Abel, S. J., Barrett, P., Brown, P., George, R., Freitag, S., McNaughton, C., Howell, S., Shank, L., Kapustin, V., Brekhovskikh, V., Kleinman, L., Lee, Y. N., Springston, S., Toniazzo, T., Krejci, R., Fochesatto, J., Shaw, G., Krecl, P., Brooks, B., McMeeking, G., Bower, K. N., Williams, P. I., Crosier, J., Crawford, I., Connolly, P., Allan, J. D., Covert, D., Bandy, A. R., Russell, L. M., Trembath, J., Bart, M., McQuaid, J. B., Wang, J., and Chand, D.: South East Pacific atmospheric composition and variability sampled along 20° S during VOCALS-REx, Atmos. Chem. Phys., 11(11), 5237–5262, doi:10.5194/acp-11-5237-2011, 2011.

Christophe, Y., Schulz, M., Bennouna, Y., Eskes, H. J., Basart, S., Benedictow, A., Blechschmidt, A.-M., Chabrillat, S., Clark, H., Cuevas, E., Flentje, H., Hansen, K. M., Im, U., Kapsomenakis, J., Langerock, B., Petersen, K., Richter, A., Sudarchikova,

https://doi.org/10.5194/acp-2019-821
Preprint. Discussion started: 8 October 2019

Atmospheric Chemistry and Physics Discussions

435 N., Thouret, V., A. Wagner, Wang, Y., Warneke, T., and Zerefos, C.: Validation report of the CAMS global reanalysis of aerosols and reactive gases, years 2003-2018, Copernicus Atmosphere Monitoring Service (CAMS) report., 2019.

Cook, P. A., Savage, N. H., Turquety, S., Carver, G. D., O'Connor, F. M., Heckel, A., Stewart, D., Whalley, L. K., Parker, A. E., Schlager, H., Singh, H. B., Avery, M. A., Sachse, G. W., Brune, W., Richter, A., Burrows, J. P., Purvis, R. M., Lewis, A. C., Reeves, C. E., Monks, P. S., Levine, J. G., and Pyle, J. A.: Forest fire plumes over the North Atlantic: p-TOMCAT model

440 simulations with aircraft and satellite measurements from the ITOP/ICARTT campaign, J. Geophys. Res. Atmos., 112(D10), 1–20, doi:10.1029/2006jd007563, 2007.

Emmons, L. K., Hauglustaine, D. A., Müller, J. F., Carroll, M. A., Brasseur, G. P., Brunner, D., Staehelin, J., Thouret, V., and Marenco, A.: Data composites of airborne observations of tropospheric ozone and its precursors, J. Geophys. Res. Atmos., 105(D16), 20497–20538, doi:10.1029/2000JD900232, 2000.

445 Eskes, H., Huijnen, V., Arola, A., Benedictow, A., Blechschmidt, A. M., Botek, E., Boucher, O., Bouarar, I., Chabrillat, S., Cuevas, E., Engelen, R., Flentje, H., Gaudel, A., Griesfeller, J., Jones, L., Kapsomenakis, J., Katragkou, E., Kinne, S., Langerock, B., Razinger, M., Richter, A., Schultz, M., Schulz, M., Sudarchikova, N., Thouret, V., Vrekoussis, M., Wagner, A., and Zerefos, C.: Validation of reactive gases and aerosols in the MACC global analysis and forecast system, Geosci. Model Dev., 8(11), 3523–3543, doi:10.5194/gmd-8-3523-2015, 2015.

450 Eskes, H. J., Bennouna, Y., Schulz, M., Christophe, Y., Basart, S., Benedictow, A., Blechschmidt, A.-M., Chabrillat, S., Clark, H., Cuevas, E., Flentje, H., Hansen, K. M., Im, U., Kapsomenakis, J., Langerock, B., Petersen, K., Richter, A., Sudarchikova, N., Thouret, V., Wagner, A., Wang, Y., and Zerefos, C.: Validation report of the CAMS global reanalysis of aerosols and reactive gases, years 2003-2016, Copernicus Atmosphere Monitoring Service (CAMS) report., 2018.

Fehsenfeld, F. C., Ancellet, G., Bates, T. S., Goldstein, A. H., Hardesty, R. M., Honrath, R., Law, K. S., Lewis, A. C., Leaitch,

455 R., McKeen, S., Meagher, J., Parrish, D. D., Pszenny, A. A. P., Russell, P. B., Schlager, H., Seinfeld, J., Talbot, R., and Zbinden, R.: International Consortium for Atmospheric Research on Transport and Transformation (ICARTT): North America to Europe - Overview of the 2004 summer field study, J. Geophys. Res. Atmos., 111(23), doi:10.1029/2006JD007829, 2006.

Flemming, J., Inness, A., Flentje, H., Huijnen, V., Moinat, P., Schultz, M. G., and Stein, O.: Coupling global chemistry transport models to ECMWF's integrated forecast system, Geosci. Model Dev., 2(2), 253–265, doi:10.5194/gmd-2-253-2009,

460 2009.

Flemming, J., Huijnen, V., Arteta, J., Bechtold, P., Beljaars, A., Blechschmidt, A. M., Diamantakis, M., Engelen, R. J., Gaudel, A., Inness, A., Jones, L., Josse, B., Katragkou, E., Marecal, V., Peuch, V. H., Richter, A., Schultz, M. G., Stein, O., and Tsikerdekis, A.: Tropospheric chemistry in the integrated forecasting system of ECMWF, Geosci. Model Dev., 8(4), 975–1003, doi:10.5194/gmd-8-975-2015, 2015.

465 Flemming, J., Benedetti, A., Inness, A., Engelen J, R., Jones, L., Huijnen, V., Remy, S., Parrington, M., Suttie, M., Bozzo, A., Peuch, V. H., Akritidis, D., and Katragkou, E.: The CAMS interim reanalysis of carbon monoxide, ozone and aerosol for 2003-2015, Atmos. Chem. Phys., 17(3), 1945–1983, doi:10.5194/acp-17-1945-2017, 2017.

https://doi.org/10.5194/acp-2019-821
Preprint. Discussion started: 8 October 2019

Atmospheric Chemistry and Physics Discussions

Fortems-Cheiney, A., Chevallier, F., Pison, I., Bousquet, P., Szopa, S., Deeter, M. N., and Clerbaux, C.: Ten years of CO emissions as seen from Measurements of Pollution in the Troposphere (MOPITT), J. Geophys. Res. Atmos., 116(5), 1–17, doi:10.1029/2010JD014416, 2011.

Inness, A., Baier, F., Benedetti, A., Bouarar, I., Chabrillat, S., Clark, H., Clerbaux, C., Coheur, P., Engelen, R. J., Errera, Q., Flemming, J., George, M., Granier, C., Hadji-Lazaro, J., Huijnen, V., Hurtmans, D., Jones, L., Kaiser, J. W., Kapsomenakis, J., Lefever, K., Leitão, J., Razinger, M., Richter, A., Schultz, M. G., Simmons, A. J., Suttie, M., Stein, O., Thépaut, J. N., Thouret, V., Vrekoussis, M., and Zerefos, C.: The MACC reanalysis: An 8 yr data set of atmospheric composition, Atmos. Chem. Phys., 13(8), 4073–4109, doi:10.5194/acp-13-4073-2013, 2013.

Inness, A., Ades, M., Agusti-Panareda, A., Barré, J., Benedictow, A., Blechschmidt, A. M., Dominguez, J., Engelen, R., Eskes, H. J., Flemming, J., Huijnen, V., Jones, L., Kipling, Z., Massart, S., Parrington, M., Peuch, V.-H., Razinger, M., Remy, S., Schulz, M., and Suttie, M.: The CAMS reanalysis of atmospheric composition, Atmos. Chem. Phys. Discuss., (January), 1–55, 2019.

Jacob, D. J.: Heterogeneous chemistry and tropospheric ozone, Atmos. Environ., 34(12–14), 2131–2159, doi:10.1016/S1352-2310(99)00462-8, 2000.

Jacob, D. J., Crawford, J. H., Maring, H., Clarke, A. D., Dibb, J. E., Emmons, L. K., Ferrare, R. A., Hostetler, C. A., Russell, P. B., Singh, H. B., Thompson, A. M., Shaw, G. E., McCauley, E., Pederson, J. R., and Fisher, J. A.: The arctic research of the composition of the troposphere from aircraft and satellites (ARCTAS) mission: Design, execution, and first results, Atmos. Chem. Phys., 10(11), 5191–5212, doi:10.5194/acp-10-5191-2010, 2010.

Lebel, T., Parker, D. J., Flamant, C., Bourlès, B., Marticorena, B., Mougin, E., Peugeot, C., Diedhiou, A., Haywood, J. M., Ngamini, J. B., Polcher, J., Redelsperger, J. L., and Thorncroft, C. D.: The AMMA field campaigns: Multiscale and multidisciplinary observations in the West African region, Q. J. R. Meteorol. Soc., 136(SUPPL. 1), 8–33, doi:10.1002/qj.486, 2010.

Lelieveld, J. and Dentener, F. J.: What controls tropospheric ozone?, J. Geophys. Res. Atmos., 105(D3), 3531–3551, doi:10.1029/1999JD901011, 2000.

Molina, L. T., Madronich, S., Gaffney, J. S., Apel, E., De Foy, B., Fast, J., Ferrare, R., Herndon, S., Jimenez, J. L., Lamb, B., Osornio-Vargas, A. R., Russell, P., Schauer, J. J., Stevens, P. S., Volkamer, R., and Zavala, M.: An overview of the MILAGRO 2006 Campaign: Mexico City emissions and their transport and transformation, Atmos. Chem. Phys., 10(18), 8697–8760, doi:10.5194/acp-10-8697-2010, 2010.

Murphy, D. M. and Fahey, D. W.: An estimate of the flux of stratospheric reactive nitrogen and ozone into the troposphere, 99(D3), 5325–5332, 1994.

Paris, J.-D., Ciais, P., Nédélec, P., Ramonet, M., Belan, B. D., Arshinov, M. Y., Golitsyn, G. S., Granberg, I., Stohl, A., Cayez, G., Athier, G., Boumard, F., and Cousin, J.-M.: The YAK-AEROSIB transcontinental aircraft campaigns: new insights on the transport of CO_2, CO and O_3 across Siberia, Tellus B, 60(5651), 551–568, doi:10.1111/j.1600-0889.2008.00369.x, 2008.

https://doi.org/10.5194/acp-2019-821
Preprint. Discussion started: 8 October 2019

Atmospheric Chemistry and Physics Discussions

Paris, J. D., Ciais, P., Nédélec, P., Stohl, A., Belan, B. D., Arshinov, M. Y., Carouge, C., Golitsyn, G. S., and Granberg, I. G.: New insights on the chemical composition of the Siberian air shed from the YAK-AEROSIB aircraft campaigns, Bull. Am. Meteorol. Soc., 91(5), 625–641, doi:10.1175/2009BAMS2663.1, 2010.

Pressman, J. and Warneck, P.: The stratosphere as a chemical sink for carbon monoxide, J. Atmos. Sci., 155–163, 1970.

Saunois, M., Reeves, C. E., Mari, C. H., Murphy, J. G., Stewart, D. J., Mills, G. P., Oram, D. E., and Purvis, R. M.: Factors controlling the distribution of ozone in the West African lower troposphere during the AMMA (African Monsoon Multidisciplinary Analysis) wet season campaign, Atmos. Chem. Phys., 9(16), 6135–6155, doi:10.5194/acp-9-6135-2009, 2009.

Sheel, V., Bisht, J. S. H., Sahu, L., and Thouret, V. R.: Spatio-temporal variability of CO and O_3 in Hyderabad (17 °N, 78 °E), central India, based on MOZAIC and TES observations and WRF-Chem and MOZART-4 models, Tellus, Ser. B Chem. Phys. Meteorol., 68(1), doi:10.3402/tellusb.v68.30545, 2016.

Singh, H. B., Brune, W. H., Crawford, J. H., Jacob, D. J., and Russell, P. B.: Overview of the summer 2004 Intercontinental Chemical Transport Experiment-North America (INTEX-A), J. Geophys. Res. Atmos., 111(24), doi:10.1029/2006JD007905, 2006.

Singh, H. B., Brune, W. H., Crawford, J. H., Flocke, F., and Jacob, D. J.: Chemistry and transport of pollution over the Gulf of Mexico and the Pacific: Spring 2006 INTEX-B campaign overview and first results, Atmos. Chem. Phys., 9(7), 2301–2318, doi:10.5194/acp-9-2301-2009, 2009.

Stein, O., Flemming, J., Inness, A., Kaiser, J. W., and Schultz, M. G.: Global reactive gases forecasts and reanalysis in the MACC project, J. Integr. Environ. Sci., 9(SUPPL. 1), 57–70, doi:10.5478/MSL.2014.5.1.12, 2012.

Wagner, A., Bennouna, Y., Basart, S., Benedictow, A., Blechschmidt, A., and Brasseur, G.: Comprehensive evaluation of the Copernicus Monitoring Service (CAMS) reanalysis against observations Atmosphere independent, 2019.

Wespes, C., Hurtmans, D., Herbin, H., Barret, B., Turquety, S., Hadji-Lazaro, J., Clerbaux, C., and Coheur, P. F.: First global distributions of nitric acid in the troposphere and the stratosphere derived from infrared satellite measurements, J. Geophys. Res. Atmos., 112(13), 1–10, doi:10.1029/2006JD008202, 2007.

Wofsy, S. C., Daube, B. C., Jimenez, R., Kort, E., Pittman, J. V., Park, S., Commane, R., Xiang, B., Santoni, G., Jacob, D., Fisher, J., Pickett-Heaps, C., Wang, H., Wecht, K., Wang, Q.-Q., Stephens, B. B., Shertz, S., Watt, A. S., Romashkin, P., Campos, T., Haggerty, J., Cooper, W. A., Rogers, D., Beaton, S., Hendershot, R., Elkins, J. W., Fahey, D. W., Gao, R. S., Moore, F., Montzka, S. A., Schwarz, J. P., Perring, A. E., Hurst, D., Miller, B. R., Sweeney, C., Oltmans, S., Nance, D., Hintsa, E., Dutton, G., Watts, L. A., Spackman, J. R., Rosenlof, K. H., Ray, E. A., Hall, B., Zondlo, M. A., Diao, M., Keeling, R., Bent, J., Atlas, E. L., Lueb, R., and Mahoney, M. J.: HIPPO Combined Discrete Flask and GC Sample GHG , Halocarbon , and Hydrocarbon Data (R _ 20121129), Analysis Center, Oak Ridge National Laboratory, Oak Ridge, Tennessee, U.S.A. [online] Available from: http://dx.doi.org/10.3334/CDIAC/hippo_012, 2012.

https://doi.org/10.5194/acp-2019-821
Preprint. Discussion started: 8 October 2019

Atmospheric Chemistry and Physics Discussions

535 **Table 1. Key setups of the three reanalyses**

Reanalysis	MACCRA	CIRA	CAMSRA
period	2003-2012	2003-2018	2003-present
Spatial resolution	80 km	110 km	80 km
Vertical resolution	60 levels	60 levels	60 levels
Temporal resolution	6-hourly analysis fields 3-hourly forecast fields from 0 UTC up to 24 hours	6-hourly analysis fields 3-hourly forecast fields from 6 and 18 UTC up to 12 hours	3-hourly analysis fields 3-hourly forecast fields from 0 UTC up to 48 hours
Assimilation system	IFS Cycle 36r1 4D-Var	IFS Cycle 40r2 4D-Var (2003-2015) & IFS Cycle 41r1 4D-Var (2016-)	IFS Cycle 42r1 4D-Var
Chemistry module	MOZART3	CB05 & Cariolle ozone parameterization in stratosphere	CB05 with updates & Cariolle ozone parameterization in stratosphere
Anthropogenic emissions	MACCity	MACCity & CO emission upgrade (Stein et al., 2014)	MACCity & CO emission upgrade (Stein et al., 2014)
Biogenic emissions	monthly mean VOC emissions by MEGAN2.1 (Guenther et al., 2006) for the year 2003	monthly mean VOC emissions by MEGAN2.1 using MERRA reanalysis meteorology for 2003-2010; a climatology dataset of the MEGAN-MACC for 2011-2017	monthly mean VOC emissions by MEGAN2.1 using MERRA reanalysis meteorology for the whole period
Biomass burning emissions	GFED (2003-2008) & GFAS v0 (2009-2012)	GFAS v1.2	GFAS v1.2

Table 2. The satellite datasets of trace gases assimilated in CAMSRA.

Species	O_3 (stratosphere)	O_3 (UTLS)	O_3 (free troposphere)	CO (free troposphere)	CO (surface/PBL)	NO_2 (free troposphere)
Satellites	MIPAS, MLS, SCIAMACHY, GOME-2A, GOME-2B, OMI, SBUV-2	Indirectly constrained by limb and nadir sounders	Indirectly constrained by limb and nadir sounders	MOPITT	Indirectly constrained by satellite IR sounders	SCIAMACHY, OMI, GOME-2

Table 3. List of used aircraft campaigns

Campaign	Date	Location	Species used	Webpage
INTEX-A	2004.07-08	East America	O_3, CO, NO, NO_2, OH, HO_2, HCHO, H_2O_2, HNO_3, PAN, C_2H_4, C_2H_6, C_3H_8, CH_3OH, CH_3COCH_3, CH_3OOH, C_2H_5OH	https://www-air.larc.nasa.gov/missions/intexna/intexna.htm
NEAQS-ITCT	2004.07-08	East America	O_3, CO	https://www.esrl.noaa.gov/csd/projects/2004/
ITOP-UK	2004.07-08	North Atlantic	O_3, CO	http://artefacts.ceda.ac.uk/badc_datadocs/itop/itop.html

https://doi.org/10.5194/acp-2019-821
Preprint. Discussion started: 8 October 2019

Atmospheric Chemistry and Physics Discussions

INTEX-B	2006.03-05	West America	O_3, CO, NO, NO_2, OH, HO_2, HCHO, H_2O_2, HNO_3, PAN, C_2H_4, C_2H_6, C_3H_8, CH_3OH, CH_3COCH_3, CH_3OOH, C_2H_5OH	https://www-air.larc.nasa.gov/missions/intex-b/intexb.html
AMMA-UK	2006.07-08	West Africa	O_3, CO	http://artefacts.ceda.ac.uk/badc_datadocs/amma/amma.html
ARCTAS	2008.04-07	North America to Arctic	O_3, CO, NO, NO_2, OH, HO_2, HCHO, H_2O_2, HNO_3, PAN, C_2H_4, C_2H_6, C_3H_8, CH_3OH, CH_3COCH_3, CH_3OOH	https://www-air.larc.nasa.gov/missions/arctas/arctas.html
VOCALS	2008.10-11	Southeast Pacific	O_3, CO	http://data.eol.ucar.edu/project/VOCALS
YAK-AEROSIB	2006-2008, 2014	Russia	O_3, CO	https://yak-aerosib.lsce.ipsl.fr/doku.php
HIPPO	2009-2011	Pacific	O_3, CO	https://hippo.ornl.gov/data_access
KORUS-AQ	2016.04-06	Korea	O_3, CO	https://www-air.larc.nasa.gov/missions/korus-aq/index.html

Table 4. Linear regression of ozone between observations and models

	All data						Troposphere data (>350 hPa)					
	N	*MB*	*MAE*	R^2	slope	*RMSE*	*N*	*MB*	*MAE*	R^2	slope	*RMSE*
MACCRA	19522	0.59	13.01	0.9291	1.02	26.064	16009	0.21	9.13	0.6145	0.71	11.705
CIRA	22308	-1.87	12.71	0.9298	0.94	22.472	18782	-2.95	9.58	0.6498	0.67	11.232
CIRA (2003-2012)	19522	-1.18	12.67	0.9341	0.94	23.225	16009	-2.29	8.99	0.6111	0.66	10.823
CAMSRA	22308	1.92	11.90	0.9375	0.94	21.174	18782	1.01	8.77	0.6927	0.72	10.996
CAMSRA (2003-2012)	19522	2.49	11.97	0.9412	0.94	21.889	16009	1.55	8.32	0.6608	0.72	10.608
Control	22308	-3.89	13.46	0.8935	0.84	25.398	18782	-1.68	9.18	0.6687	0.66	10.611
Control (2003-2012)	19522	-3.71	13.72	0.8966	0.85	26.662	16009	-1.08	8.76	0.6229	0.63	10.155

Note: N is the number of points considered for the calculation of the correlation, *MB* the mean bias (expressed in ppb), *MAE* the mean absolute error (expressed in ppb), *R* the correlation coefficient and *RMSE* the root mean square error (expressed in ppb).

Table 5. Linear regression of CO between the aircraft campaign observations and the reanalyses

	All data						Data < 300 ppb					
	N	*MB*	*MAE*	R^2	slope	*RMSE*	*N*	*MB*	*MAE*	R^2	slope	*RMSE*
MACCRA	18376	-10.40	27.13	0.2005	0.30	54.921	17972	-5.96	18.69	0.5992	0.63	23.346
CIRA	21353	-6.55	28.56	0.3990	0.49	60.912	20254	-2.48	17.72	0.6775	0.72	25.052
CIRA (2003-2012)	18376	-4.86	23.71	0.3573	0.42	51.397	17894	-1.65	16.25	0.6588	0.70	22.900

https://doi.org/10.5194/acp-2019-821
Preprint. Discussion started: 8 October 2019

Atmospheric Chemistry and Physics Discussions

CAMSRA	21353	-6.85	29.23	0.3559	0.49	66.706	20233	-3.82	17.34	0.7061	0.78	25.284
CAMSRA (2003-2012)	18376	-5.42	25.26	0.2716	0.40	60.387	17869	-3.21	16.04	0.6863	0.77	23.553
Control	21353	-0.11	31.78	0.3565	0.50	68.489	20187	2.45	20.15	0.6588	0.75	27.013
Control (2003-2012)	18376	-0.25	27.74	0.2746	0.41	60.123	17881	2.03	19.11	0.6234	0.71	24.920

Note: N is the number of points considered for the calculation of the correlation, *MB* the mean bias (expressed in ppb), *MAE* the mean absolute error (expressed in ppb), *R* the correlation coefficient and *RMSE* the root mean square error (expressed in ppb).

Table 6. Qualitative summary of the over- and under-estimation by the CAMSRA for several observed chemicals at 4 geographic locations and at two altitudes (6 km and surface)

	At 6 km				surface			
	Arctic	Bangor	Hawaii	Mexico-City	Arctic	Bangor	Hawaii	Mexico-City
O_3	G	G	G	O	OO	O	G	O
CO	G	U	G	U	G	O	U	O
NOx	UU	U	U	G	U	OO	O	O
OH	UU	O	G	G	UU	O	O	G
HO_2	O	O	G	O	U	O	G	O
H_2O_2	UU	U	G	G	UU	G	O	OO
HNO_3	UU	U	UU	G	U	O	U	O
PAN	U	U	O	OO	O	OO	OO	OO
C_2H_4	U	G	UU	UU	U	OO	O	G
C_2H_6	UU	UU	U	U	UU	UU	UU	UU
C_3H_8	UU	UU	U	U	UU	UU	UU	UU
HCHO	UU	UU	U	U	UU	U	G	O
CH_3OH	UU	U	U	G	O	O	G	OO
CH_3COCH_3	UU	UU	UU	UU	UU	G	UU	U
C_2H_5OH	UU	UU		UU	UU	O		U
CH_3OOH		UU	U	U		G	U	OO

Note: G = -10 % < bias < 10 %; O = 10 % < bias < 40 %; U = -40 % < bias < -10 %; OO = bias > 40 %; UU = bias < -40 %.

https://doi.org/10.5194/acp-2019-821
Preprint. Discussion started: 8 October 2019

Atmospheric Chemistry and Physics Discussions

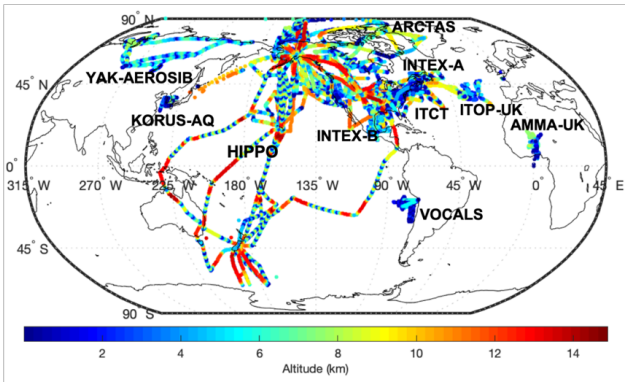

570

Figure 1. Flight tracks of the campaigns with the altitude of the corresponding flight.

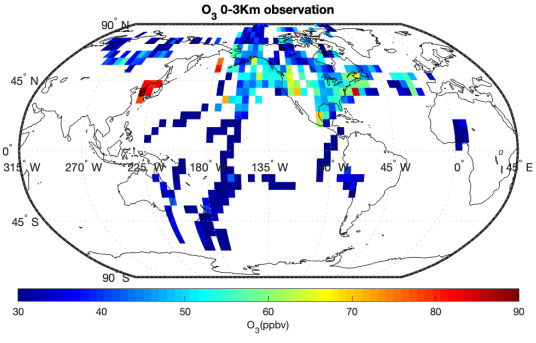

https://doi.org/10.5194/acp-2019-821
Preprint. Discussion started: 8 October 2019

Atmospheric Chemistry and Physics Discussions

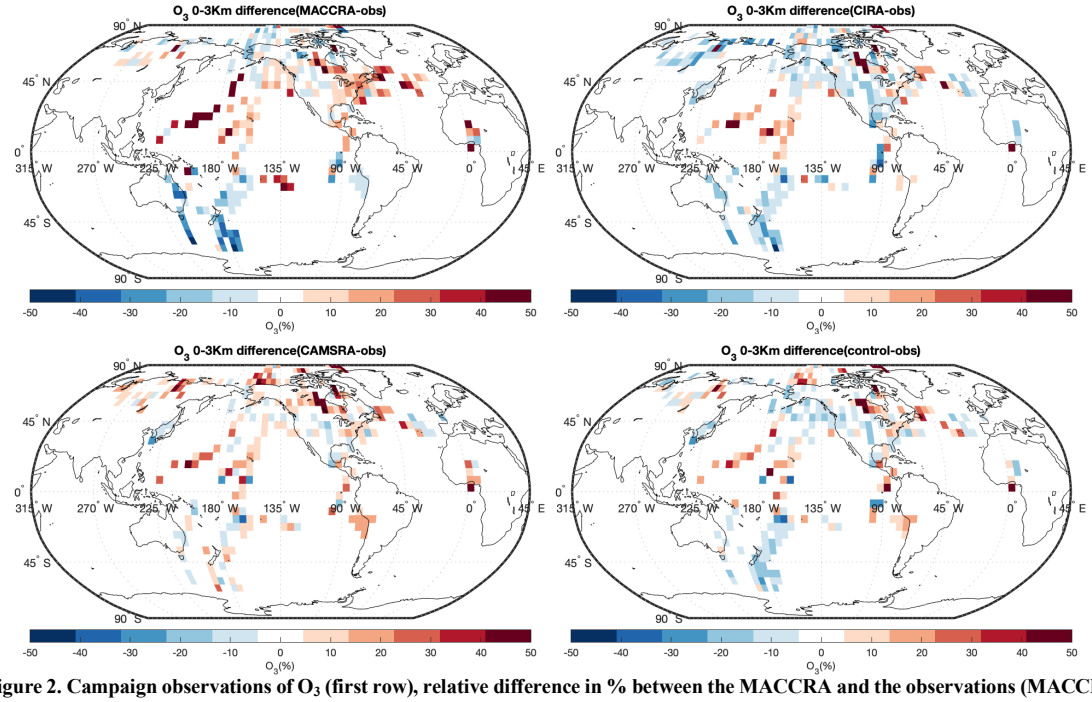

Figure 2. Campaign observations of O_3 (first row), relative difference in % between the MACCRA and the observations (MACCRA – observation; left of second row), difference between the CIRA and the observation (CIRA – observation; right of second row), difference between the CAMSRA and the observation (CAMSRA – observation; left of third row), and the difference between the control run and the observation (control – observation; right of third row). The data are averaged to 5°×5° (latitude × longitude) and to the altitude bin of 0-3 km. Note that MACCRA only includes campaigns between 2003-2012.

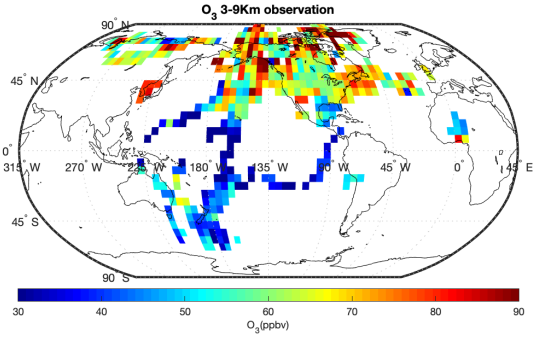

https://doi.org/10.5194/acp-2019-821
Preprint. Discussion started: 8 October 2019

Atmospheric Chemistry and Physics Discussions

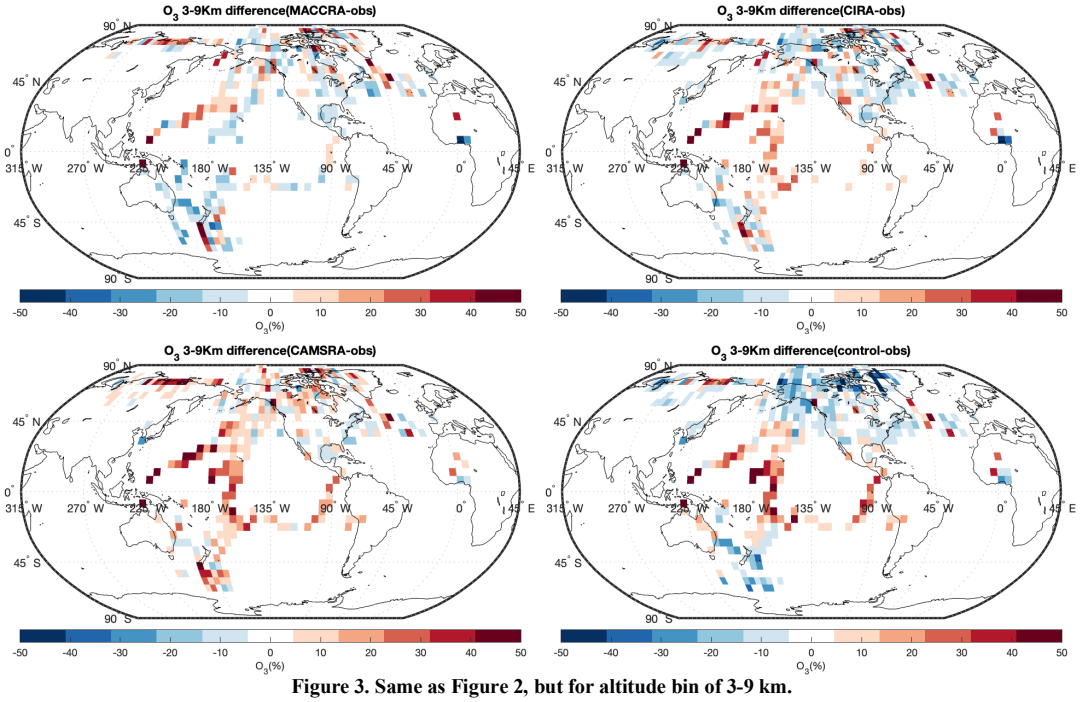

585 **Figure 3. Same as Figure 2, but for altitude bin of 3-9 km.**

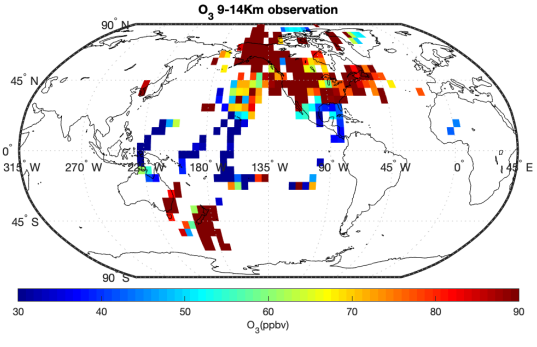

https://doi.org/10.5194/acp-2019-821
Preprint. Discussion started: 8 October 2019

Atmospheric Chemistry and Physics Discussions

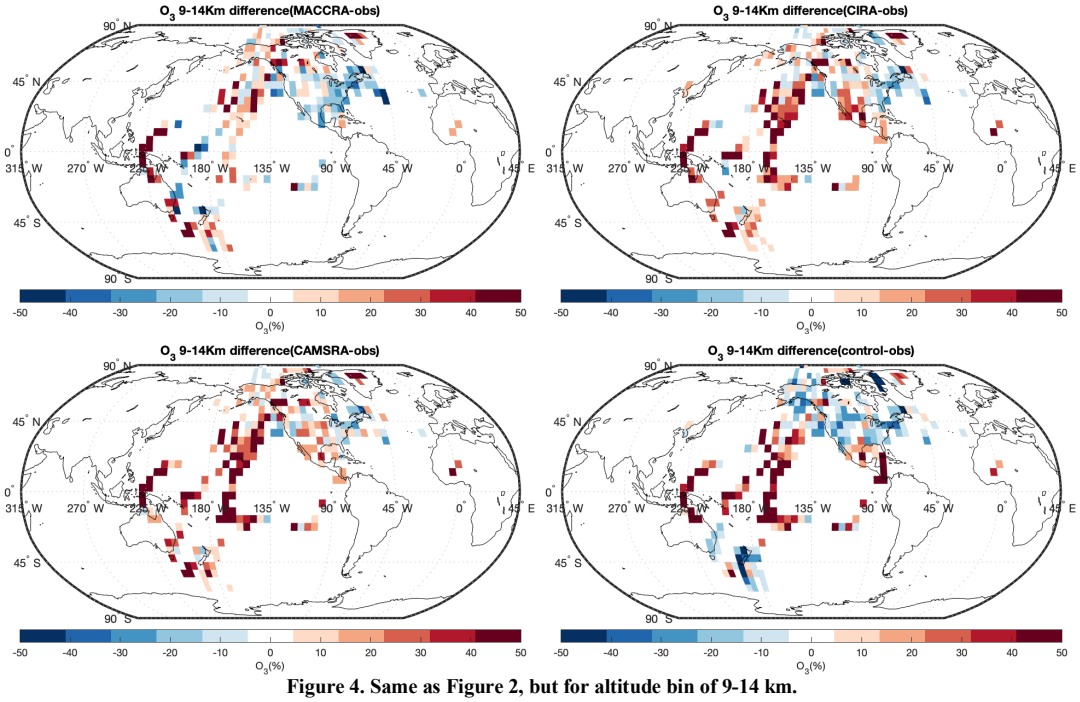

590 **Figure 4. Same as Figure 2, but for altitude bin of 9-14 km.**

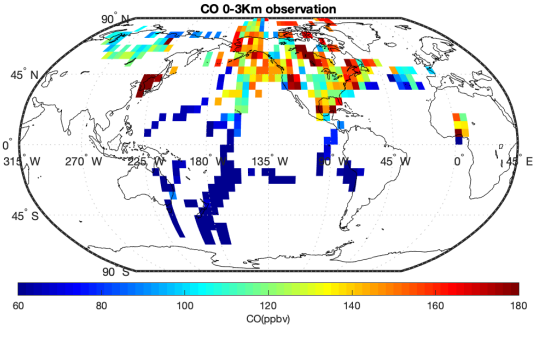

https://doi.org/10.5194/acp-2019-821
Preprint. Discussion started: 8 October 2019

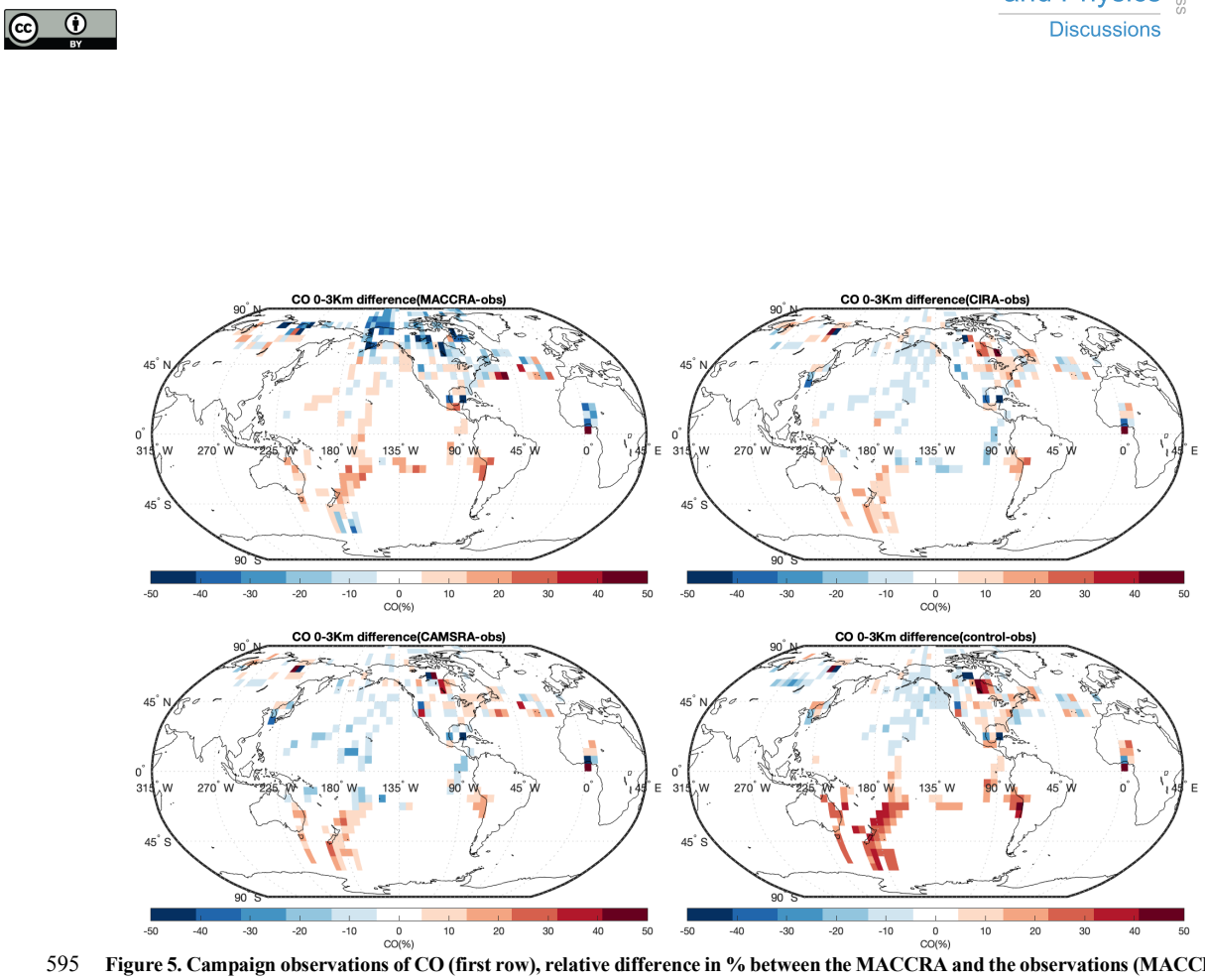

595 **Figure 5. Campaign observations of CO (first row), relative difference in % between the MACCRA and the observations (MACCRA – observation; left of second row), difference between the CIRA and the observation (CIRA – observation; right of second row), difference between the CAMSRA and the observation (CAMSRA – observation; left of third row), and the difference between the control run and the observation (control – observation; right of third row). The data are averaged to 5°×5° (latitude × longitude) and to the altitude bin of 0-3 km.**

600

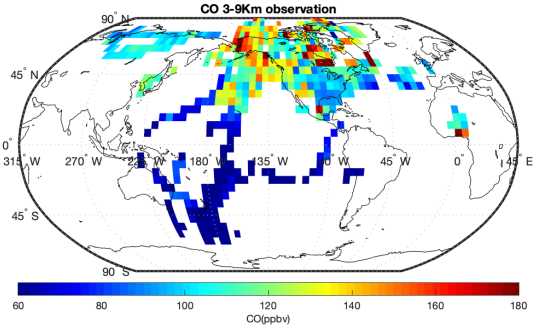

https://doi.org/10.5194/acp-2019-821
Preprint. Discussion started: 8 October 2019

Atmospheric Chemistry and Physics Discussions

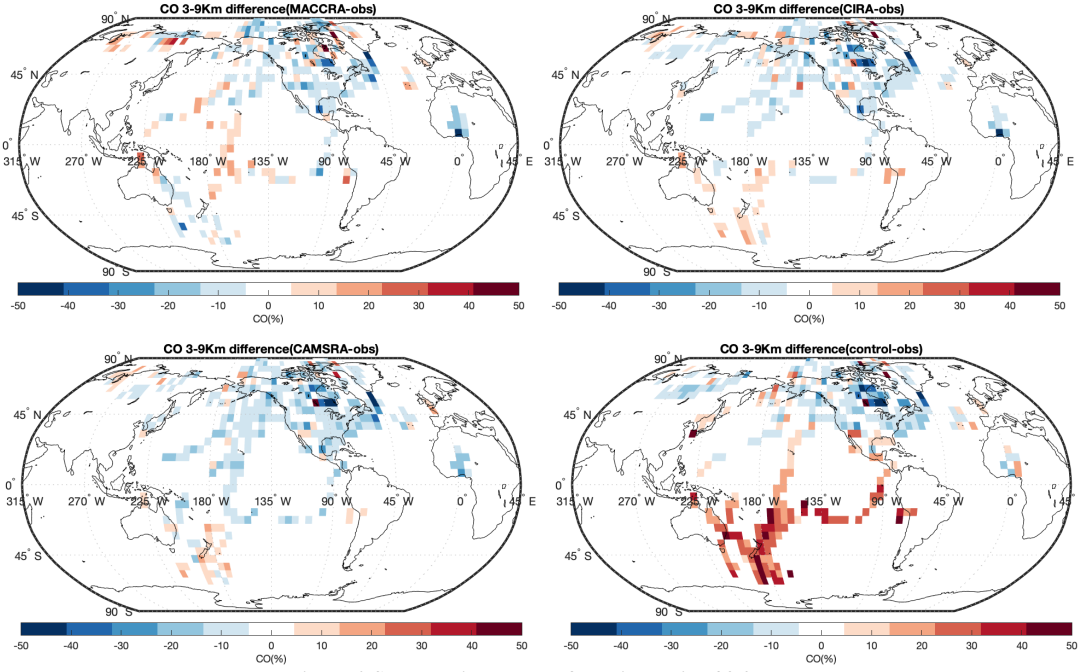

Figure 6. Same as Figure 5, but for altitude bin of 3-9 km.

605

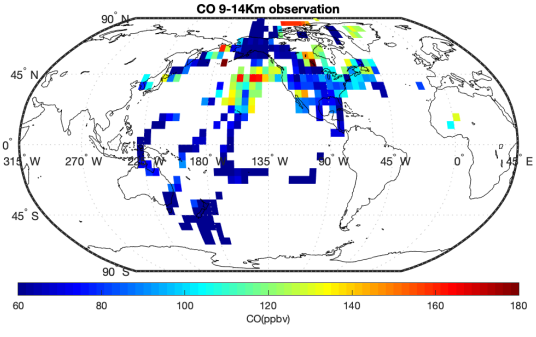

https://doi.org/10.5194/acp-2019-821
Preprint. Discussion started: 8 October 2019

Atmospheric Chemistry and Physics Discussions

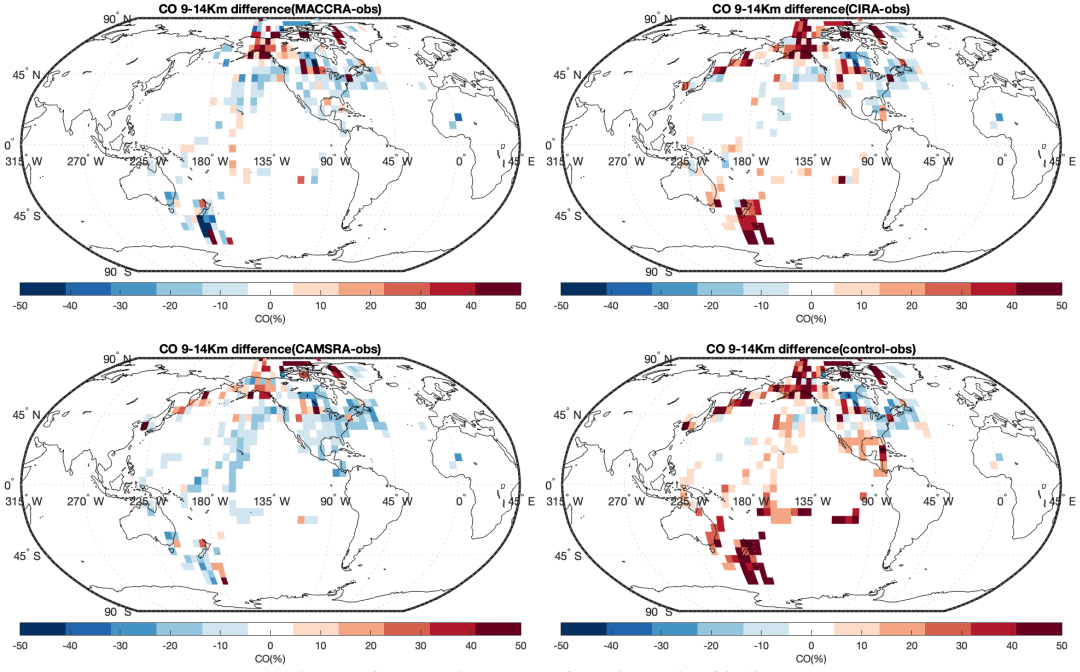

Figure 7. Same as Figure 5, but for latitude bin of 9-14 km.

610

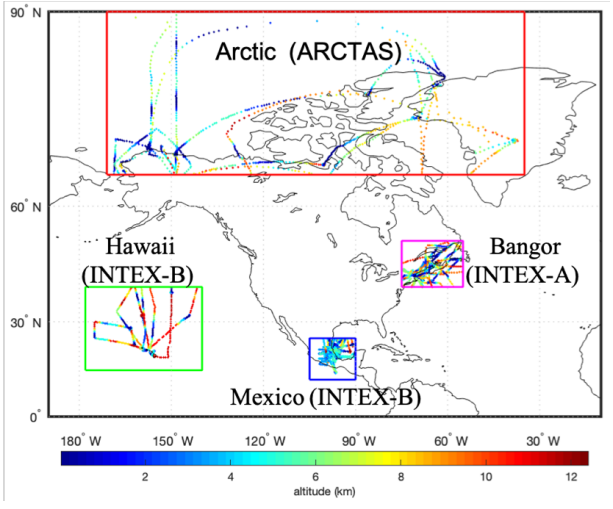

Figure 8. The location of the four selected regions. The red, green, blue, and magenta rectangles show the Arctic (ARCTAS, 2008.04-07), Hawaii (INTEX-B, 2006.03-05), Mexico (INTEX-B, 2006.03-05), and Bangor (INTEX-A, 2004.07-08), respectively.

https://doi.org/10.5194/acp-2019-821
Preprint. Discussion started: 8 October 2019

Atmospheric Chemistry and Physics Discussions

615

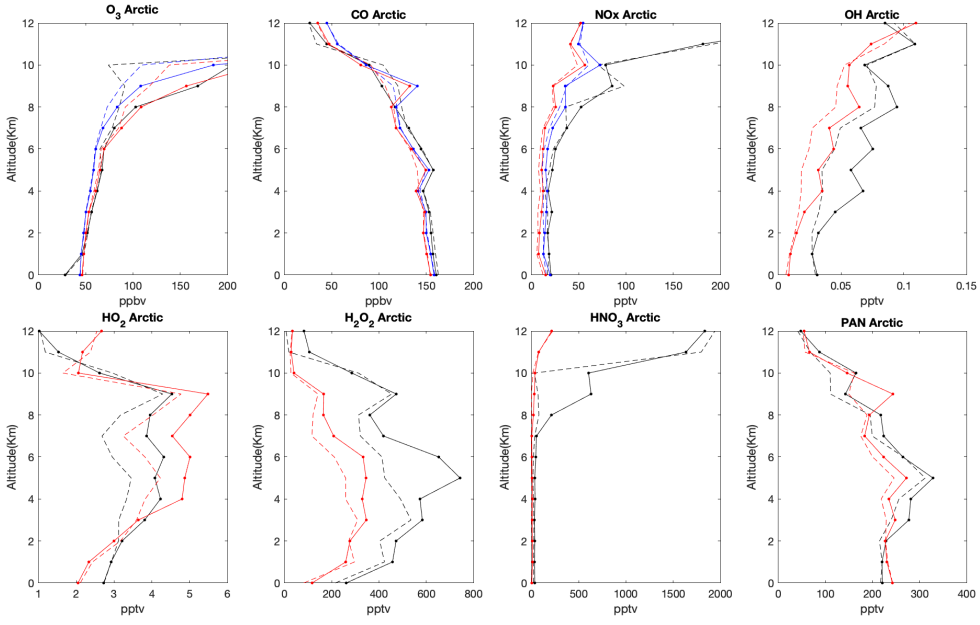

620

https://doi.org/10.5194/acp-2019-821
Preprint. Discussion started: 8 October 2019

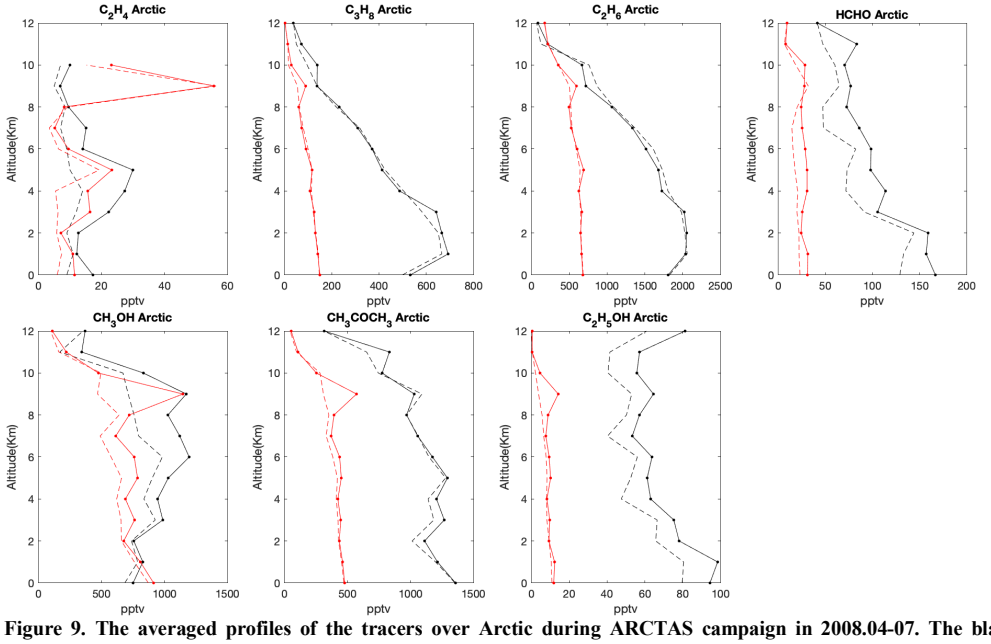

Figure 9. The averaged profiles of the tracers over Arctic during ARCTAS campaign in 2008.04-07. The black lines are the observations, the red lines are the CAMSRA, and the blue lines are the control run (only shown for O_3, CO and NO_X). The solid lines are the mean profiles, and the dash lines are the median profiles.

https://doi.org/10.5194/acp-2019-821
Preprint. Discussion started: 8 October 2019

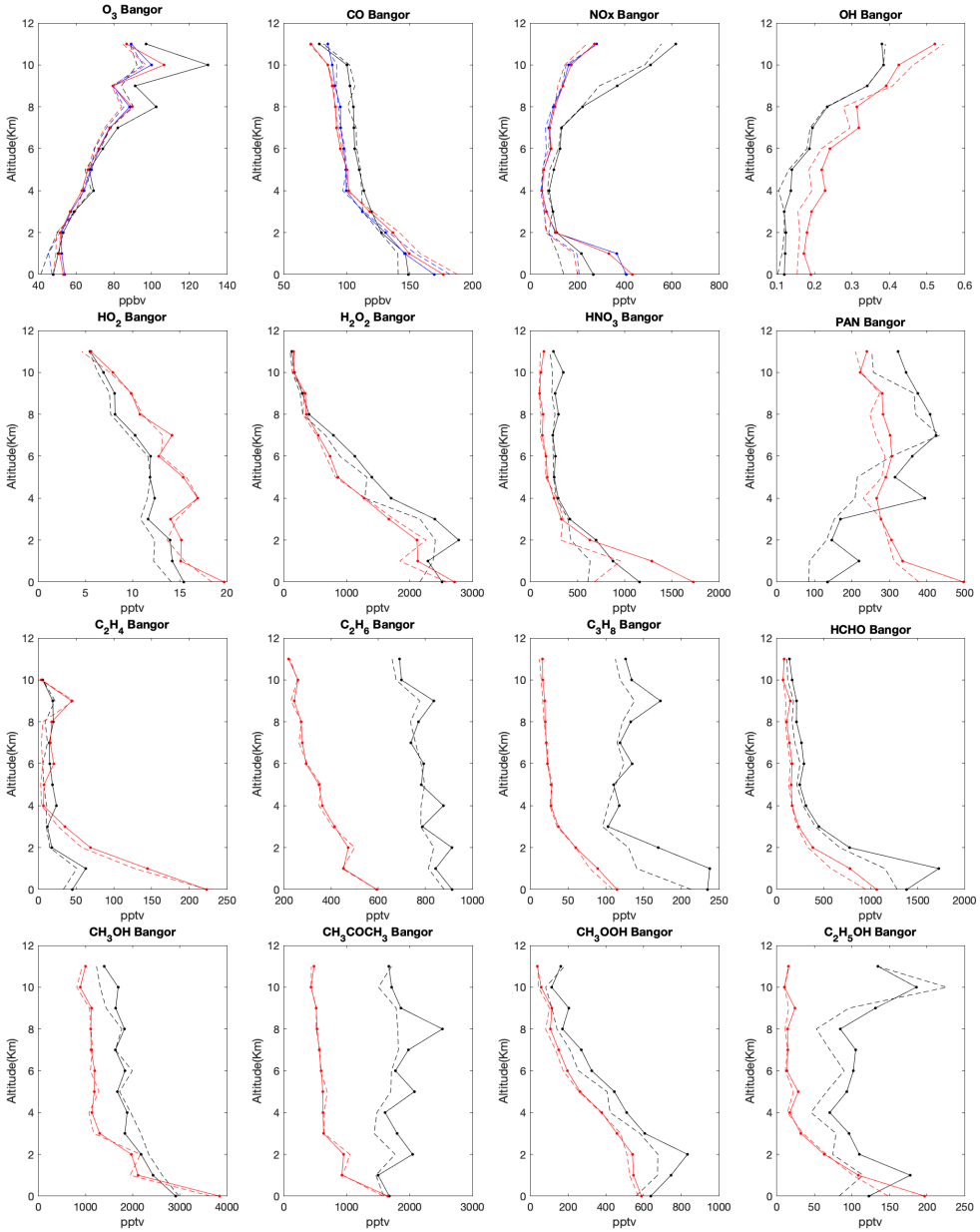

Figure 10. The same as figure 9, but for Bangor during campaign INTEX-A in 2004.07-08.

https://doi.org/10.5194/acp-2019-821
Preprint. Discussion started: 8 October 2019

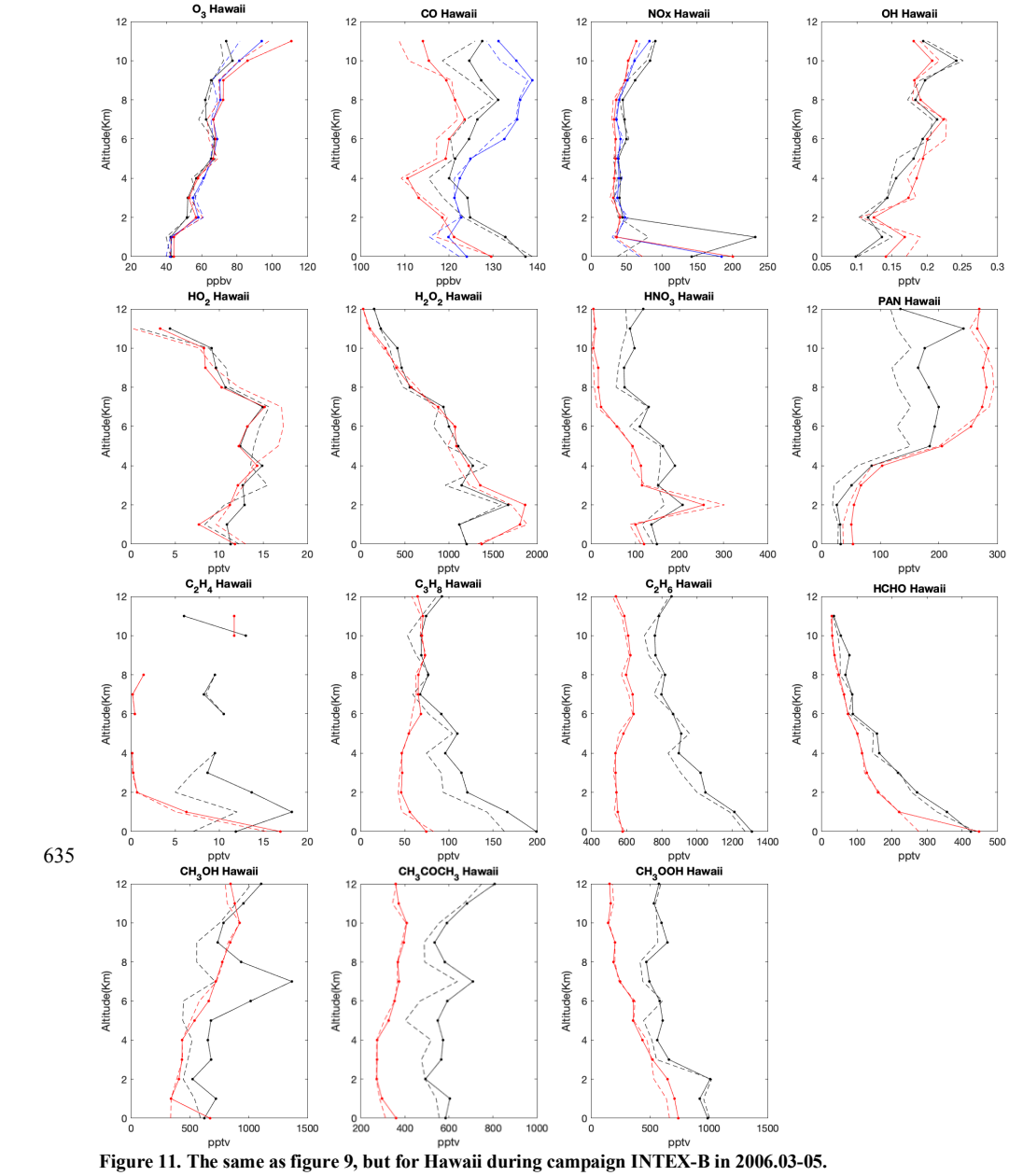

Figure 11. The same as figure 9, but for Hawaii during campaign INTEX-B in 2006.03-05.

https://doi.org/10.5194/acp-2019-821
Preprint. Discussion started: 8 October 2019

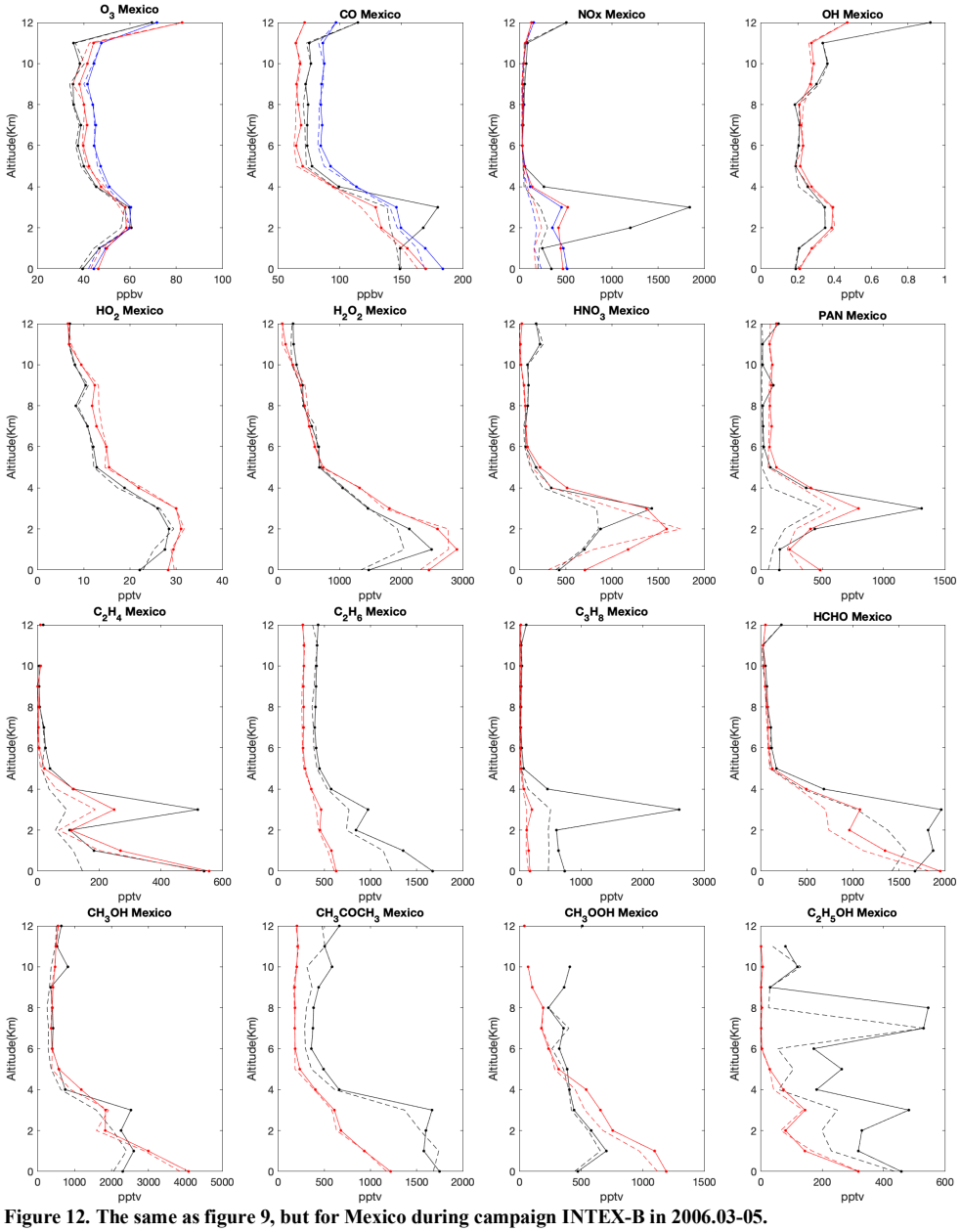

Figure 12. The same as figure 9, but for Mexico during campaign INTEX-B in 2006.03-05.

https://doi.org/10.5194/acp-2019-821
Preprint. Discussion started: 8 October 2019

Atmospheric Chemistry and Physics Discussions

Appendix

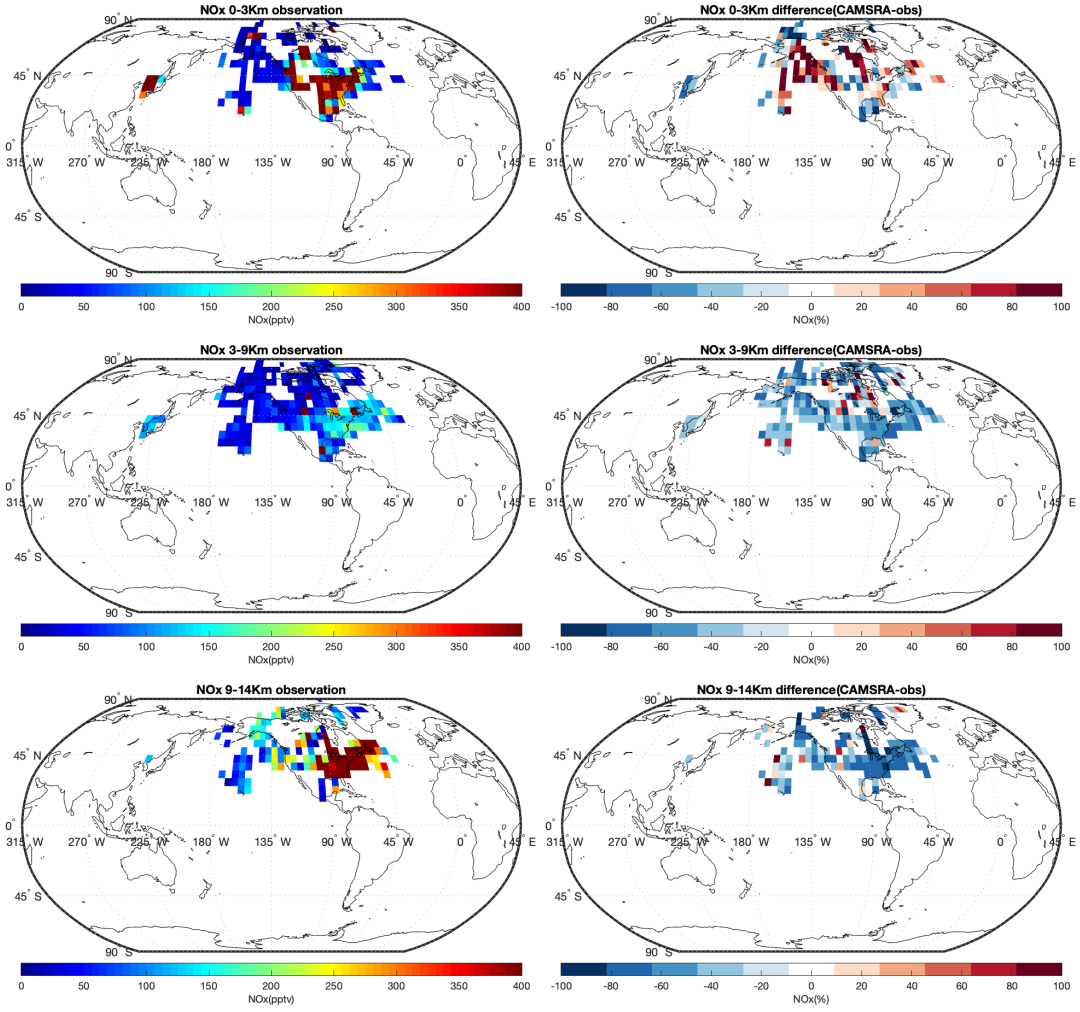

Figure A1. Campaign observations of NO_X (left panel) and the difference between the CAMSRA and the observations (difference = CAMSRA – observation; right panel). The data are averaged to 5°×5° (latitude × longitude) and to three altitude bins: 0-3 km, 3-9 km, and 9-14 km.

https://doi.org/10.5194/acp-2019-821
Preprint. Discussion started: 8 October 2019

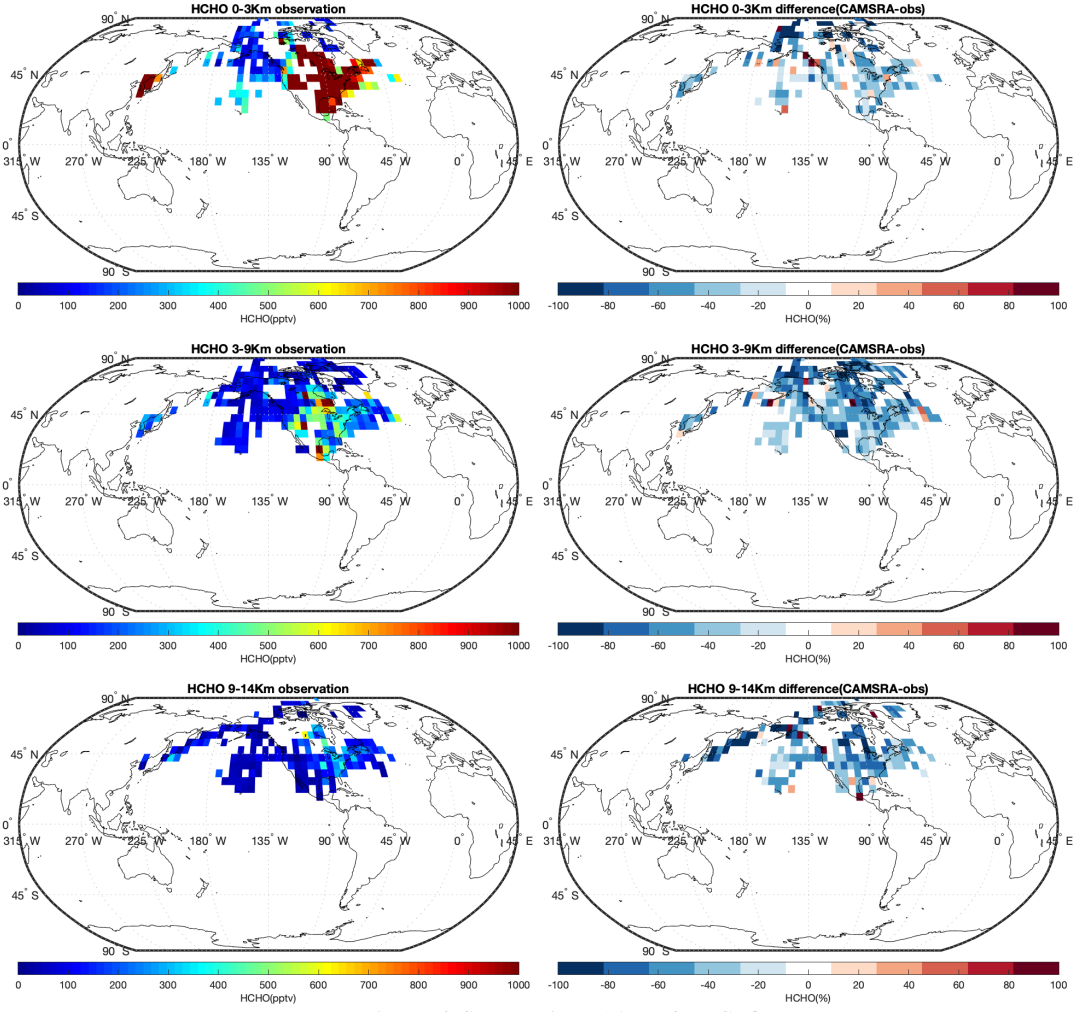

655 **Figure A2. Same as Figure A1, but for HCHO.**

https://doi.org/10.5194/acp-2019-821
Preprint. Discussion started: 8 October 2019

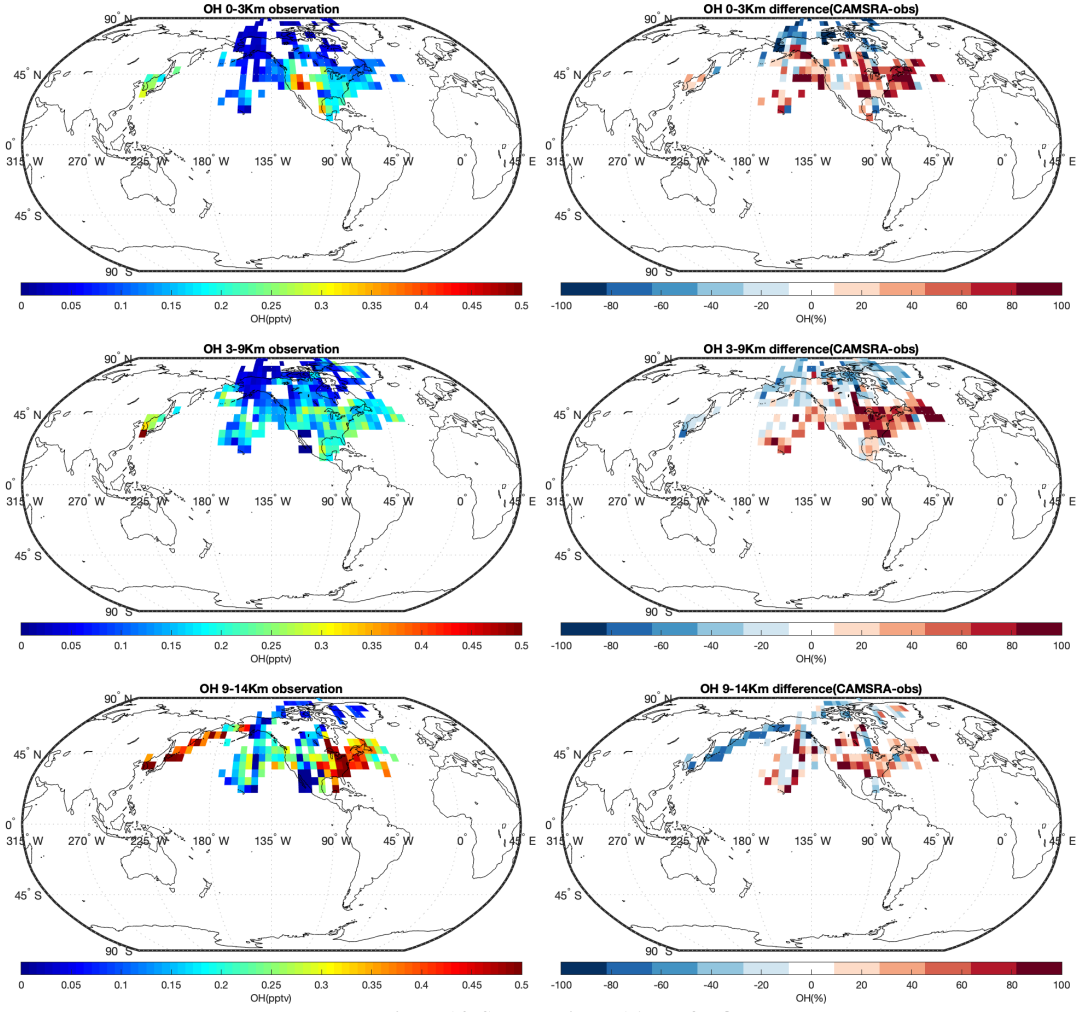

Figure A3. Same as Figure A1, but for OH.

https://doi.org/10.5194/acp-2019-821
Preprint. Discussion started: 8 October 2019

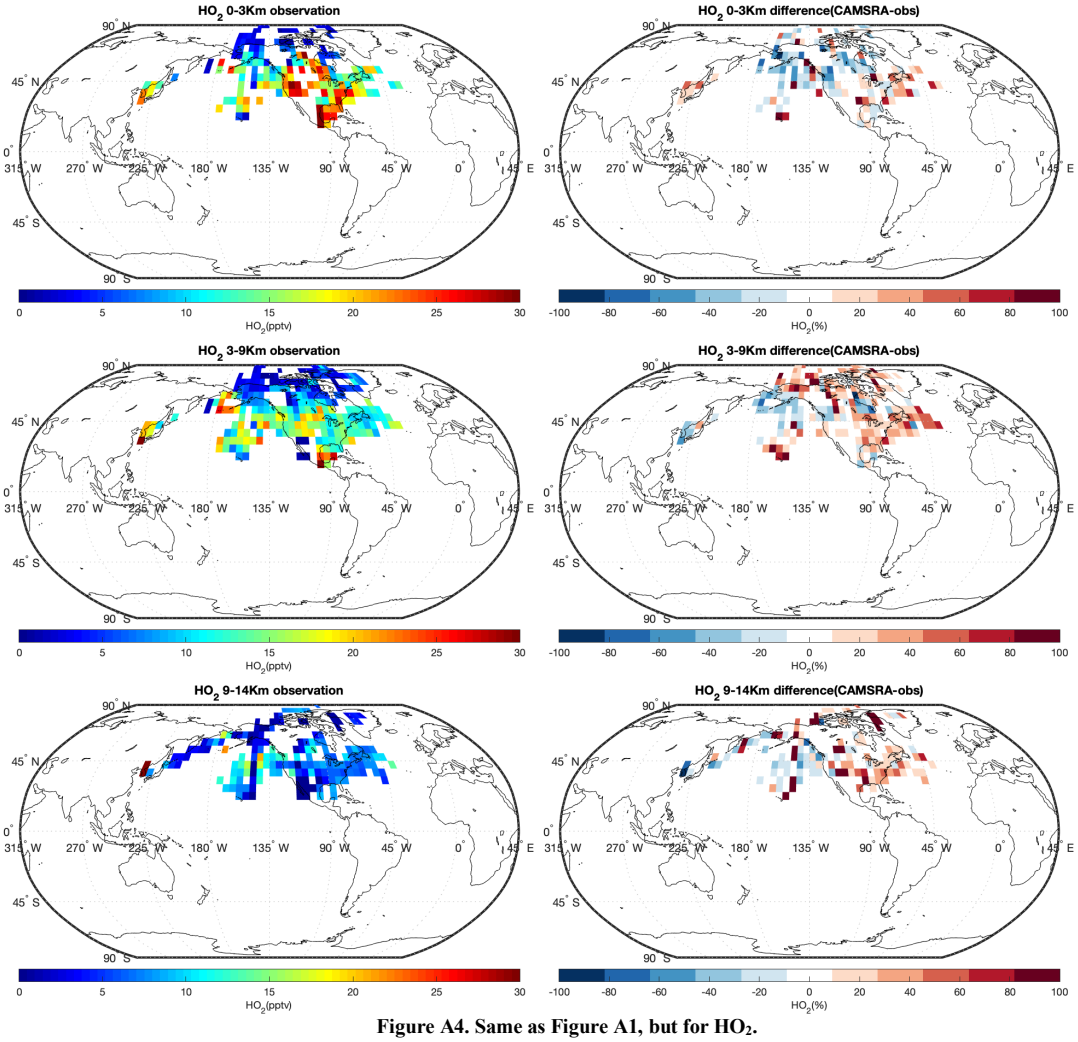

Figure A4. Same as Figure A1, but for HO_2.